

Application of electrochemical methods for the detection of abiotic stress biomarkers in plants

Li, Zhilei^{1,2}; Zhou, Jianping¹; Dong, Tao^{1,3}; Xu, Yan; Shang, Yukui¹

¹College of Mechanical Engineering, Xinjiang University, China

²Engineering Training Center of Xinjiang University, China

³Department of Microsystems (IMS), Faculty of Technology, Natural Sciences and Maritime Sciences, University of South-Eastern Norway

This is an Accepted Manuscript of an article published by Elsevier in *Biosensors and Bioelectronics* on March 30, 2021, version of record:

<https://doi.org/10.1016/j.bios.2021.113105>

Li, Z., Zhou, J., Dong, T., Xu, Y., & Shang, Y. (2021). Application of electrochemical methods for the detection of abiotic stress biomarkers in plants. *Biosensors and Bioelectronics*, 182, Article 113105. <https://doi.org/10.1016/j.bios.2021.113105>



Except where otherwise noted, this item's license is described as Attribution- NonCommercial-NoDerivatives 4.0 Internasjonal

Application of electrochemical methods for the detection of abiotic stress biomarkers in plants

Zhilei Li ^{a,b}, Jianping Zhou ^{a,*}, Tao Dong ^{c,**}, Yan Xu ^a, Yukui Shang ^a

^a College of Mechanical Engineering, Xinjiang University, Urumchi, 830047, China

^b Engineering Training Center of Xinjiang University, Urumchi, 830047, China

^c Department of Microsystems (IMS), Faculty of Technology, Natural Sciences and Maritime Sciences, University of South-Eastern Norway, Postboks 235, 3603, Kongsberg, Norway

Abstract:

Abiotic stress is the main cause of low productivity in plants. Therefore, it is important to detect stress and respond to it in a timely manner to avoid irreversible damage to plant productivity and health. The application of traditional methods in agriculture is limited by expensive equipment and cumbersome sample processing. More effective detection methods are urgently needed due to the trace amounts and low stabilities of plant biomarkers. Electrochemical detection methods have the unique advantages of high accuracy, a low detection limit, fast response and easy integration with systems. In this review, the application of three types of electrochemical methods to phytohormone assessment is highlighted, including direct electrochemical, immunoelectrochemical, and photoelectrochemical methods. Research on electrochemical methods for detecting abiotic stress biomarkers, including various phytohormones, is also summarized with examples. To date, the detection limit of exogenous plant hormones can reach pg/mL or even lower. Nevertheless, more efforts need to be made to develop a portable instrument for in situ online detection if electrochemical sensors are to be applied to the detection of endogenous hormones or the physiological state of plants. Additionally, plant-wearable sensors that can be directly attached to or implanted into plants for continuous, noninvasive and real-time monitoring are emphasized. Finally, rational summaries of the considered methods and present challenges and future prospects in the field of abiotic stress detection-based electrochemical biosensors are thoroughly discussed.

Key Words: abiotic stress; phytohormone; electrochemical sensor; real-time detection; invasive detection

0. Introduction

In addition to growing in greenhouse environments, most plants grow in relatively rough outdoor environments, so they are often subjected to adverse light, temperature, humidity, nutrition, and water conditions and other abiotic stress factors (Kumar et al., 2012; Wang et al., 2003; Mishra et al., 2016). These adverse conditions will affect the changes in physiological state throughout the life cycle of crops and eventually lead to a decrease in crop yield (Mishra et al., 2016; Graf and Smith, 2011; Kalaji et al., 2016; Khan et al., 2015). It has been projected that crop losses due to abiotic stresses may be as high as 70% of the yield of staple food crops (Kaur et al., 2008). In addition, this damage to plants may ultimately influence people's health. A study by a U.S. environmental action group in 2006 estimated that the toxic effects of heavy metals on plants affected more than 1 million people in eight countries (Khan et al., 2015). Plants have evolved several physiological mechanisms to cope with the adverse effects of abiotic stress. Accordingly, if intrinsic changes in the physiology, biochemistry, and molecules in plant tissues can be triggered by various abiotic stresses, then these stresses can be diagnosed in a timely manner, and protection measures can be applied to plants. Thus, the damage from stress can be reduced. In addition, understanding the status of plants in extreme surroundings is the key to achieving precision agriculture.

Following exposure to abiotic stress, to minimize damage, specific ion channels and kinase cascades will be activated, and reactive oxygen species (ROS) and phytohormones will accumulate, yielding stress-tolerance effects that help plants adapt and survive these stressful situations (Ben Rejeb et al., 2014). When plants encounter external stresses, the levels of many phytohormones will change accordingly (Hu et al., 2020). Under stress conditions, such as drought, extreme temperatures, and high salinity, the content of abscisic acid (ABA), which regulates various physiological processes, will increase considerably (Tuteja, 2007; Sah et al., 2016). Therefore, ABA is now considered a plant stress hormone (Tuteja, 2007; Vishwakarma et al., 2017). Indole-3-acetic acid (IAA), which is involved in almost every aspect of plant growth and development, is a ubiquitous phytohormone. It plays an important role in the response to salt stress and drought stress in crop plants (Fahad et al., 2015; H. Li et al., 2019; Hu et al., 2020; Sun et al., 2018). Salicylic acid (SA), a phenolic compound, regulates growth and responses to biotic and abiotic stress by modulating the production of various osmolytes and secondary metabolites (Khan et al., 2015). Jasmonates (JAs)

and ethylene (ET) often crosstalk with one another when providing defense in regard to the abiotic stress tolerance of the plant. JAs, ET and their signaling pathways can differentially regulate the stress tolerance of plants in a species-specific manner (Kazan, 2015).

Therefore, researchers can monitor abiotic stress responses in plants by detecting the phytohormones caused by sophisticated signaling and protective systems (Mishra et al., 2016). Considering that plant hormones can have direct and/or indirect effects on multiple plant functions (Kazan, 2015), it is necessary to measure several substances simultaneously to understand the crosstalk between different molecules.

1. Detection methods of phytohormones

The earliest method used to detect plant biomarkers was a bioassay, which has been utilized as a reporter system combined with paper chromatography or thin-layer chromatography (Thimann and Skoog, 1940). However, it is nonspecific. In early studies, IAA and related substances were detected by specific color reactions after they were separated using paper chromatography or thin-layer chromatography (Ueda and Bandurski, 1969). Currently, these methods are not used singly to detect IAA, but together with high-performance liquid chromatography (HPLC) or high-performance thin-layer chromatography (HPTLC). Immunological techniques such as radioimmunoassay (Pengelly, 1977) and immunocytochemistry (Dewitte and Van Onckelen, 2001) have been used to quantify endogenous auxin, but due to their unstable test results and use of expensive antibodies, these qualification methods are not widely used. Modern analytical techniques, such as capillary electrophoresis with fluorescence detection (Olsson et al., 1998; Chen et al., 2011), share the same procedures as traditional methods, including extraction, pretreatment, resolution (separation by chromatography, capillary electrophoresis, gas chromatography (GC), HPLC or ultra-performance liquid chromatography (UPLC)) and detection (detection of signals by UV monitoring, fluorescence monitoring, mass spectrometry (MS) or tandem mass spectrometry (MS/MS)) (Seo et al., 2016). Plant biomarker phytohormones have been determined by HPLC coupled with MS (Hou et al., 2008; Ma et al., 2008; Wrkruprh et al., 2001), fluorescence (Lu et al., 2010; G. Li et al., 2015), chemiluminescence (Xi et al., 2009), GC/MS (Vine et al., 1987; Müller et al., 2002; Schmelz et al., 2003), and enzyme-linked immunosorbent assay (ELISA), which relies on high-quality antibodies and is susceptible to impurities (Li et al., 2003). GC, HPLC or UPLC combined with MS/MS are currently the strongest tools to simultaneously identify and quantify auxin- and auxin-related substances (Seo et al., 2016). To confirm the validity of other methods, HPLC-MS is adopted as the gold standard for plant biomarker detection (Hernández et al., 1997; Hu et al., 2020; L. J. Sun et al., 2014). However, these methods require considerable time, are dependent on reagents and trained operators, and destroy the sample. In addition, they are operated in the laboratory, requiring expensive equipment that is not suitable for the in situ or in vivo monitoring of abiotic stresses in plants. To monitor the status of plant growth in a timely manner, researchers have focused on biosensors, which consist of a recognition module and a signal conversion component. The reported work has mainly focused on two aspects, including the design of an efficient biointerface (associated with the selection and preparation of materials) and the choice of the signal transformation and amplification method, which may be electrochemical or involve optical fibers or field effect transistors (FETs), among others. Electrochemistry is the most popular and mature signal transformation method due to its advantages of simplicity, rapidity, high sensitivity, low cost, and easy integration. A summary of the developments in plant hormone electrochemical sensors, including direct electrochemical, immunoelectrochemical, photoelectrochemical (PEC), and molecular imprinting electrochemical sensors, will be discussed below.

2. Electrochemical sensors for phytohormones

2.1 Direct electrochemical sensors for phytohormones

2.1.1 Traditional electrochemical sensors for phytohormones

Many groups have studied the electrochemical behavior of several phytohormones. Direct electrochemical sensors using a silicone OV-17-modified carbon paste electrode and carbon fiber ultramicroelectrode (CFUMEs) were proposed by researchers at the Autonoma University of Madrid to directly determine the concentration of IAA (Hernández et al., 1996, 1994). The same group also quantified ABA in a hanging drop mercury electrode (HDME), which was the first electrochemical study of ABA (Hernández et al., 1996). Considering the toxicity and environmental pollution potential of mercury, Yardim applied a bismuth-coated pencil-lead graphite electrode that combined the favorable electroanalytical characteristics of a bismuth-film electrode (BiFE) with the advantage of pencil-based graphite (Yardim, 2011). Electrochemical methods have also been used for other phytohormones, such as indole-3-butyric acid (IBA) (Shen et al., 2013; Chýlková et al., 2019) and cis-jasmone (Dang et al., 2012; Dang et al., 2011). The principle of detection is the oxidation behavior of plant hormones in the appropriate media. However, the application of electrochemical sensors for plant biomarker detection is limited because some biomarkers have no or low electrochemical activity, the materials used for electrode modification have poor electrocatalytic abilities, and the surface of the electrode is easily polluted by the electrooxidation and electropolymerization of biomarkers (Gan et al., 2011; Gualandi et al., 2011; Yardim and Erez, 2011;

Yardim and Şentürk, 2011; de Toledo and Vaz, 2007; Zhang et al., 2010). Researchers have performed considerable work to improve the sensitivity of sensors and reduce their detection times. The development of nanomaterials has supported improvements in electrochemical sensor sensitivity. One recent research focus related to electrochemical sensors is the design of sensing modules that contain nanomaterials with high activity, good selectivity, a large specific surface area and small size. As shown in Table 1, many efforts have been made to detect phytohormones with electrochemical methods utilizing different nanomaterials, such as graphene (Gan et al., 2011; Feng et al., 2014), gold nanoparticles (AuNPs) (Sun et al., 2013) and carbon nanotubes (Wu et al., 2003).

2.1.1.1 In vivo or in situ detection

Because of the unstable structure of plant biomarkers such as IAA and the extra need to pretreat plant samples, there is an urgent need to develop in vivo or in situ methods to perform real-time analysis of plant biomarkers. The success of the DII-VENUS sensor developed by Brunoud et al. (Brunoud et al., 2012) suggested a strategy in which endogenous IAA in different parts of plants could be mapped in a way that was similar to the in vivo electrochemical analysis of biomarkers in animals. Recently, paper-based analytical devices (PADs) have been increasingly studied due to their low cost, ease of fabrication, and need for a low volume of sample solution (Santhiago et al., 2013; Feng et al., 2013; Sun and Johnson, 2015). L. J. Sun et al. applied PADs for the in situ electrochemical detection of SA at the ng level in live tomato leaves (L. J. Sun et al., 2014). By coupling a multiwalled carbon nanotube (MWCNT)/Nafion-modified carbon tape electrode in a PAD, the amount of SA could be detected in situ under different conditions. As shown in Figure 1, SA in tomato leaves diffused onto the carbon tape-modified electrode when phosphate buffer solution (PBS) in the filter paper passed through a hole made in a tomato leaf with a professional tool. The results obtained by this approach were validated by conventional methods such as HPLC-MS/MS, gene expression analyses and experiments on the interference of components in the sap of tomatoes, and this technique showed potential for the real-time study of chemicals in living organisms. One of the issues that restricts the application of PADs is the lack of cost-effective materials used to fabricate working electrodes. As excellent graphite resources, pencils have been used for electrode modification (Alipour et al., 2013; Gong et al., 2012; Kariuki, 2012), PADs integrated with pencil trace-modified electrodes have been reported for the detection of biomarkers (Li et al., 2016; Petrek et al., 2007; Santhiago et al., 2017; Santhiago and Kubota, 2013). The Ning Bao group at Nantong University utilized PADs modified with hand-drawn pencil traces and digitally controlled pencil traces to achieve the real-time sensing of SA in tomato leaves and *Arabidopsis thaliana* leaves, respectively (H. R. Wang et al., 2019; He et al., 2020). For data acquisition in agricultural fields, sensors have been developed with a focus on their low cost, portability, and nondestructive in situ and in vivo detection.

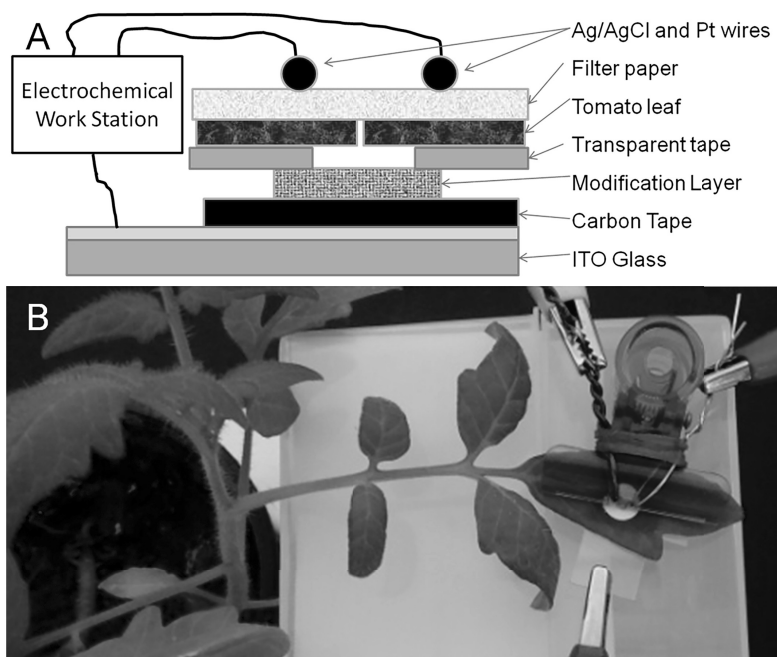


Fig. 1. Cross-sectional view (A) and real image (B) of a PAD for in situ detection of SA in a tomato leaf. Reprinted with permission from (L. J. Sun et al., 2014).

Huo and coworkers applied cost-effective stainless steel (SS) sheets as substrates to fabricate flat electrodes (Huo et al., 2020). As shown in Figure 2, the SS sheets were modified with carbon cement and then coupled in PADs for the analysis of IAA in plants. This work presented SS as an alternative material for preparing disposable carbon-based working electrodes for practical applications.

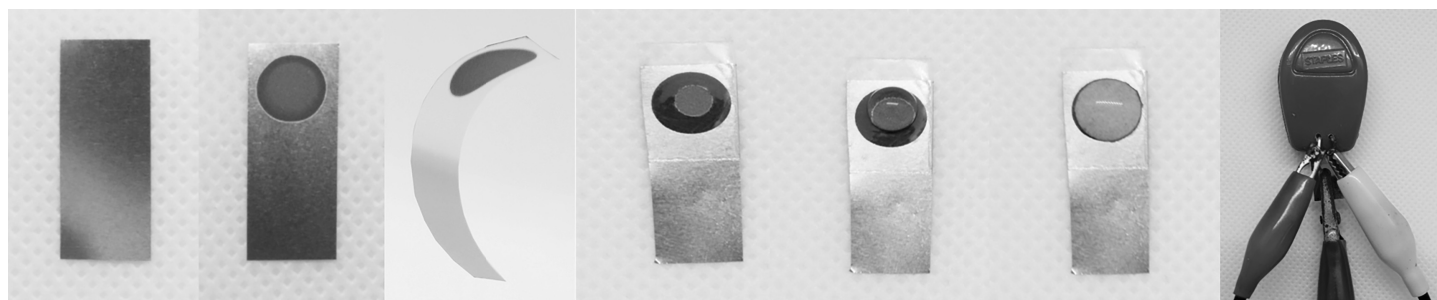


Fig. 2. Preparation of the modified SS electrode. A) SS sheet, B) SS sheet modified with carbon adhesive cement, C) bent modified SS electrode, D) definition of the effective area of the modified electrode with plastic tape with a hole, E), addition of sample solution to the modified electrode, F), application of a piece of filter paper on the surface of the modified electrode, G) clasp with a Ag/AgCl wire and a platinum wire, used to provide the reference electrode and the counter electrode. Reprinted with permission from (Huo et al., 2020).

2.1.1.2 Simultaneous detection

The response mechanism of plants to abiotic stresses depends on the crosstalk between different components of the hormonal system, which is associated with the concentration ratio of auxins to other phytohormones (Cao et al., 2019; Yardim and Şentürk, 2011); therefore, it is necessary to quantify auxins such as IAA and other phytohormones at the same time to directly and credibly study the interaction between them. Yardim and Şentürk were the first to utilize a voltammetric method to simultaneously monitor different classes of phytohormones (Yardim and Şentürk, 2011). In this work, a pencil-lead graphite (PG) electrode was fabricated to simultaneously determine the concentrations of IAA and kinetin. The amounts of IAA and SA were first simultaneously determined by Sun et al. using a MWCNT-chitosan (CS)-modified glassy carbon electrode (GCE) (Sun et al., 2015). Combining the advantages of carboxymethyl cellulose (CMC), montmorillonite (MMT) and single-walled carbon nanotubes (SWCNTs), Lu et al. prepared a CMC-MMT-SWCNT/GCE sensor to simultaneously detect two trace phytohormones (Lu et al., 2015). Taking advantage of the high specific surface area, good electron mobility, porosity, and 3D-networked structure of graphene hydrogel (GH), which is a three-dimensional (3D) graphene nanomaterial, Cao et al. developed a GH-modified GCE to simultaneously detect both IAA and SA in the range of 4 to 200 μM with a limit of detection (LOD) of 1.42 μM and 2.80 μM , respectively, by using cyclic voltammetry (CV) and linear sweep voltammetry (LSV) (Cao et al., 2019). To achieve simultaneous phytohormone detection in very small amounts of tissue with insufficient liquid for in situ monitoring, Sun et al. fabricated PADs on the basis of previous work (L. J. Sun et al., 2014) using oxygen plasma/MWCNT-modified carbon tape and plasma/graphene oxide (GO)-modified carbon tape as disposable working electrodes for seedling tissues. The concentrations of free IAA and SA in different zones of pea seedlings were obtained by collecting very small amounts (only several milligrams) of tissue with a sample punch and putting them directly on the working electrode (Sun et al., 2017; Sun et al., 2018), as shown in Figure 3 and Figure 4.

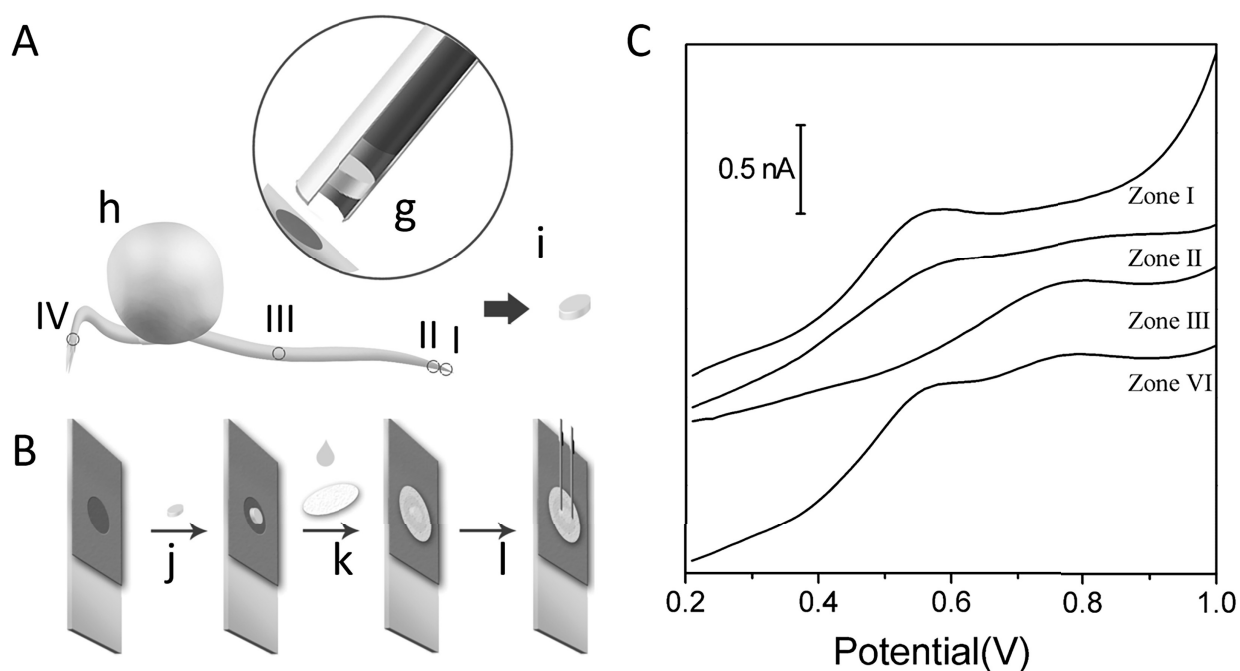


Figure 3. Sampling process (A), sample application on the surface of working electrodes (B) and typical differential pulse voltammetry (DPV) curves for Zones I, II, III, and IV (C). Very small tissue portions (i) in Zones I, II, III and IV of the pea seedling (h) were sampled with a sample punch (g). The obtained samples were then put on the surface of a modified electrode (j). Buffer solution with a volume of 10 μL was then dropped onto the electrode, and a piece of

filter paper was used to cover the electrode surface (k). A clasp with a platinum wire and a Ag/AgCl wire was used to provide the counter electrode and the reference electrode (l). Reprinted with permission from (Sun et al., 2017).

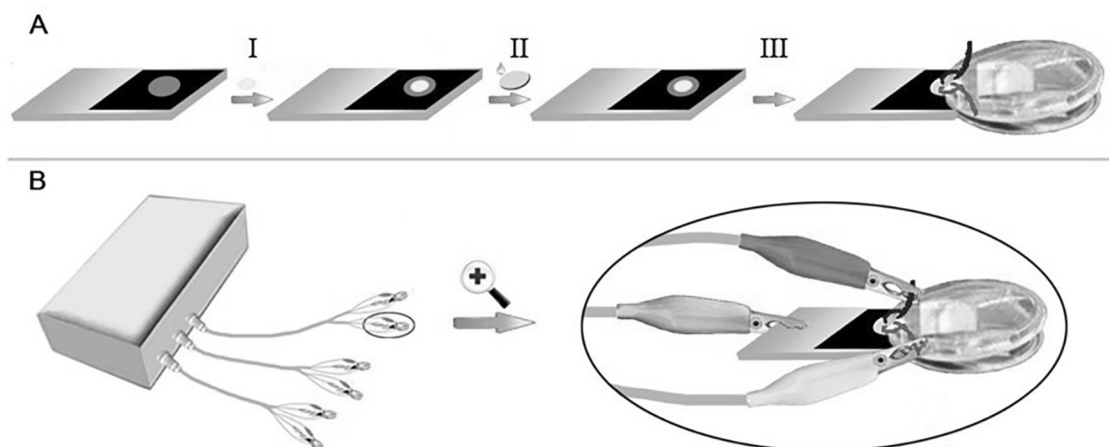


Fig. 4. A The process of applying a plant sample with a weight of several milligrams on the surface of a working electrode for detection (I), adding buffer solution with a volume of 10 μL and a piece of filter paper for covering and connection (II), and applying a clasp with a platinum wire and a Ag/AgCl wire for electrochemical detection (III). B. Detection of IAA and SA in pea seedlings with six channels of a CHI 1040 electrochemical station (eight channels in total). Reprinted with permission from (Sun et al., 2018).

2.1.2 Ratiometric electrochemical sensors

All the methods above are single-signal sensors (Gao et al., 2015), which may suffer false positive or negative errors when used in complicated detection environments (Deng et al., 2015; Yu and Lai, 2012; Zuo et al., 2009). Ratiometric electrochemical sensors have attracted the attention of researchers owing to the advantages of their dual-signaling strategies, in which an independent redox probe is introduced to offer built-in correction (Ren et al., 2015; Wu et al., 2013; Hu et al., 2020). Recently, studies have utilized ratiometric electrochemical sensors to detect biomolecules such as nucleic acids (Deng et al., 2017), proteins (Ren et al., 2015), small biological molecules (Cui et al., 2018) and metal ions (Jia et al., 2016). Recent works also show that this method can be used to simultaneously detect two parameters, such as glucose and pH (Li et al., 2017). In regard to phytohormone detection, Hu et al. built a multifunctional ratiometric sensor to simultaneously detect IAA and SA (Hu et al., 2020). The key is ferrocene (Fc), which was used as the reference substance to modify the detection results. To improve the sensitivity of the sensor, MWCNTs and carbon black (CB) were used to modify the GCE, and Nafion was applied to avoid interference from other substances.

2.2 Immunochemical sensors for phytohormones

Considering that many phytohormones are simultaneously present in plant tissues, it is urgent to develop a method with high specificity. By virtue of the specific binding of an antigen to an antibody, immunochemical sensors can effectively discriminate target analytes from other interfering substances. These sensors have been sought for use in numerous applications in the fields of clinical and biochemical analysis because of their excellent properties of high sensitivity, good selectivity, low cost, low reagent consumption, and fast response. However, the application of immunochemical sensors for detecting plant hormones is still limited to the detection of exogenous hormones. To our knowledge, portable, in vivo and in situ immunochemical sensors have not been reported.

Because plant tissues contain very few plant hormones, a high detection sensitivity is needed. The key to improving the sensitivity of immunochemical sensors is improving the stability and amount of antibody loaded on the electrode and the trapping capacity of the immunosensor for the antigen. Researchers have explored different materials as immobilization matrices to enhance the adsorption of antibodies. Li et al. (2003) described a sol-gel-alginate-carbon composite electrode based on an enzyme-linked competitive immunoreaction, in which the value of the reduction current was directly proportional to the amount of IAA bound on the electrode and inversely proportional to the amount of IAA to be measured. Similarly, Wang et al. (2009) used AuNPs to modify a GCE by virtue of their high specific surface area, good conductivity and biocompatibility. Su and coworkers prepared a porous graphene (PG) bionanocomposite by chemical prereduction and electroreduction processes. PG was combined with AuNPs and applied as the anti-IAA antibody matrix to capture IAA, as shown in Figure 5 (Su et al., 2019).

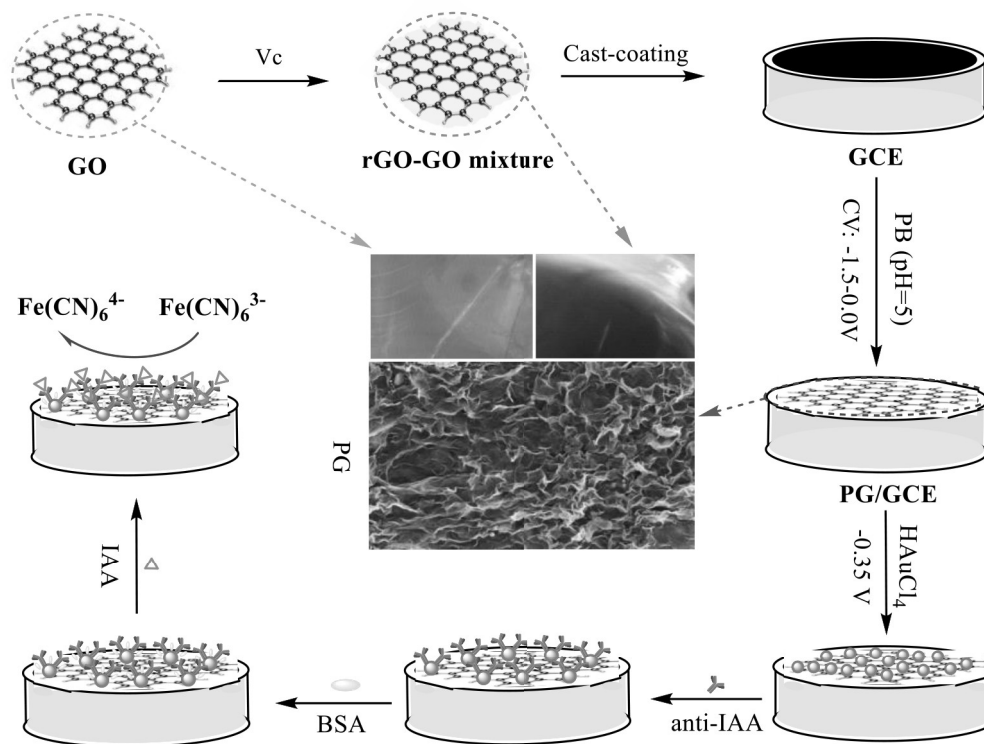


Fig. 5. Schematic illustration of the fabrication and detection process of the electrochemical immunosensor. Reprinted with permission from (Su et al., 2019).

After the formation of an immunocomplex, the electron transfer resistance of the electrode interface will increase, which will lead to an increase in impedance and a decrease in the reduction peak current of the probe. Accordingly, impedance-based biosensors and amperometric-based biosensors are listed and summarized as follows.

2.2.1 Impedance-based biosensors

An impedance immunosensor is used to study a solution or electrode matrix by electrochemical impedance spectroscopy. When the substance to be measured reacts with the modified electrode interface or solution, the conductivity of the solution or electrode film will change, and the amount of the substance to be measured can be measured by detecting these changes.

Researchers have detected ABA by monitoring the impedance of working electrodes based on the direct adsorption of the antibody on a modified electrode. As mentioned above, the stability and amount of antibody loaded on the electrode are critical problems for immunoelectrochemical sensors. The modification of biointerfaces using ideal materials is usually adopted to solve this problem. Porous gold surfaces have been increasingly studied due to their inertness, high surface area, and excellent electrical conductivity. A porous nanostructured gold film can lead to an 11.4-fold increase in thiol adsorption and a 3.3-fold increase in protein adsorption under optimized deposition conditions (Bonroy et al., 2004). Li and coworkers prepared a porous nanogold film to fix anti-ABA antibodies on a GCE through electrostatic adsorption and covalent conjugation. The linear range for the detection of ABA from hybrid rice samples was 0.5–5,000 ng/mL, and the LOD was 0.1 ng/mL (Li et al., 2008). The same group also applied an α -phenylenediamine-modified gold electrode for protein embedment by crosslinking interactions (Shi et al., 2007) in the determination of ABA (Li et al., 2010a). These immunosensors prove that an effective biological interface can adsorb enough phytohormones to generate an impedance response.

2.2.2 Amperometric-based biosensors

Amperometric-based biosensors deal with electroactive substances. These sensors work primarily by monitoring the signals of redox reactions occurring on the surface of the electrode that are catalyzed by antibody- or antigen-labeled enzymes. Enzyme-labeled amperometric-based immunosensor methods mainly include the competitive method and the sandwich method. Although electrochemical sandwich immunosensors are most widely used at present, they suffer from a fundamental limitation in that the molecule to be tested must be large enough to provide two binding sites, which is not conducive to the detection of phytohormones (g/mol). As a way to circumvent these limitations, Huanshun Yin's group at Shandong Agricultural University developed non-sandwich electrochemical immunosensors (Zhou et al., 2013; Yin et al., 2013).

The signal amplification strategy is another key factor for improving electrochemical immunosensors. Studies have applied various signal amplification units, for example, various nanomaterials, such as graphene (Tang et al., 2011; H. Yin et al., 2011b), AuNPs (H. Yin et al., 2011a; Z. Yin et al., 2011), magnetic

nanoparticles (Fe_3O_4) (H. Yin et al., 2011c; Zhang et al., 2012), copper oxide (CuO) (Li et al., 2012), and carbon nanotubes (Yin et al., 2010; Yue et al., 2012), to enhance the ability of the sensor to capture antibodies or antigens. Zhou et al. developed a non-sandwich electrochemical immunosensor for IAA in the leaves of mung bean sprouts, which is shown in Figure 6 (Zhou et al., 2013). They used graphene and AuNPs as the matrix of the signal amplification unit to assemble AuNPs functionalized with horseradish peroxidase-labeled immunoglobulin G (AuNPs-HRP-IgG), in which the volume ratio of AuNPs to IgG-HRP was 4:1. Because of the presence of AuNPs, the amount of IAA immobilized on the electrode was enhanced; thus, the linear range of this immunosensor was 1×10^{-9} to 5×10^{-6} M, and the LOD by DPV reached 5.5×10^{-10} M ($S/N = 3$). On the basis of this work, the same group introduced a double signal amplification method using Fe_3O_4 -HRP-IgG and anti-IAA-AuNPs as signal amplification probes (Figure 7) (Yin et al., 2013). Fe_3O_4 -HRP-IgG was immobilized on the electrode surface through glycosyl groups in HRP-IgG and 4-aminophenylboronic acid (APBA) and served as a trapping agent to further capture anti-IAA-AuNPs. The anti-IAA-AuNP unit was captured by Fe_3O_4 -HRP-IgG through a specific interaction between the primary antibody and secondary antibody. The linear range was from 0.02 to 500 ng/mL, and the LOD reached 0.018 ng/mL ($S/N = 3$). Su et al. was the first to apply thiolated conducting polymers (CPs) as anchors to immobilize Au to obtain a uniform dispersion of AuNPs (Su et al., 2020). In this paper, the triple signal amplification strategy of AuNPs/thiolated polypyrrole (TPPy)-PG, AuNPs-IgG and AuNPs-anti-IAA allowed for the capture of more anti-IAA and IAA biomolecules on the modified electrode surface through immunoreactions, as shown in Figure 8.

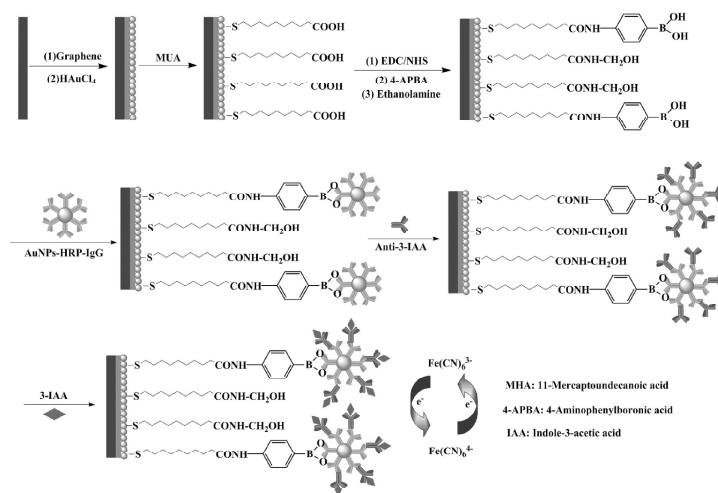


Fig. 6. Fabrication process and detection mechanism of the proposed electrochemical immunosensor. Reprinted with permission from (Zhou et al., 2013).

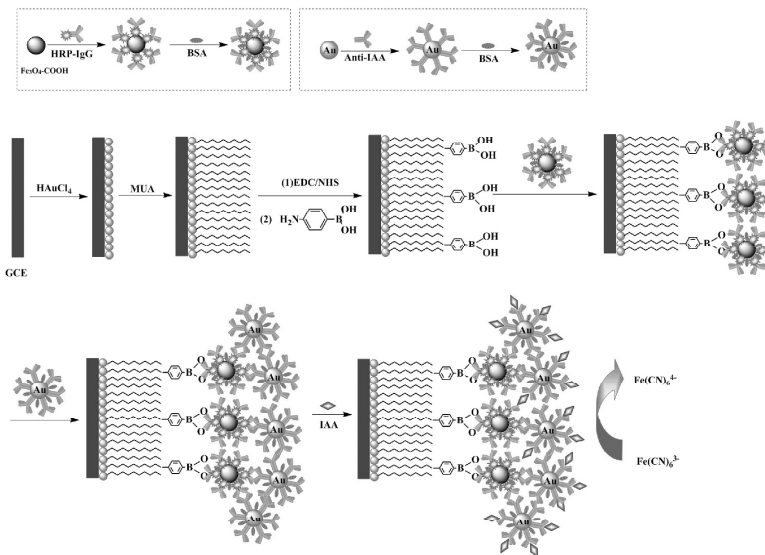


Fig. 7. Schematic illustration of the fabrication and detection process of the electrochemical immunosensor. Reprinted with permission from (Yin et al., 2013).

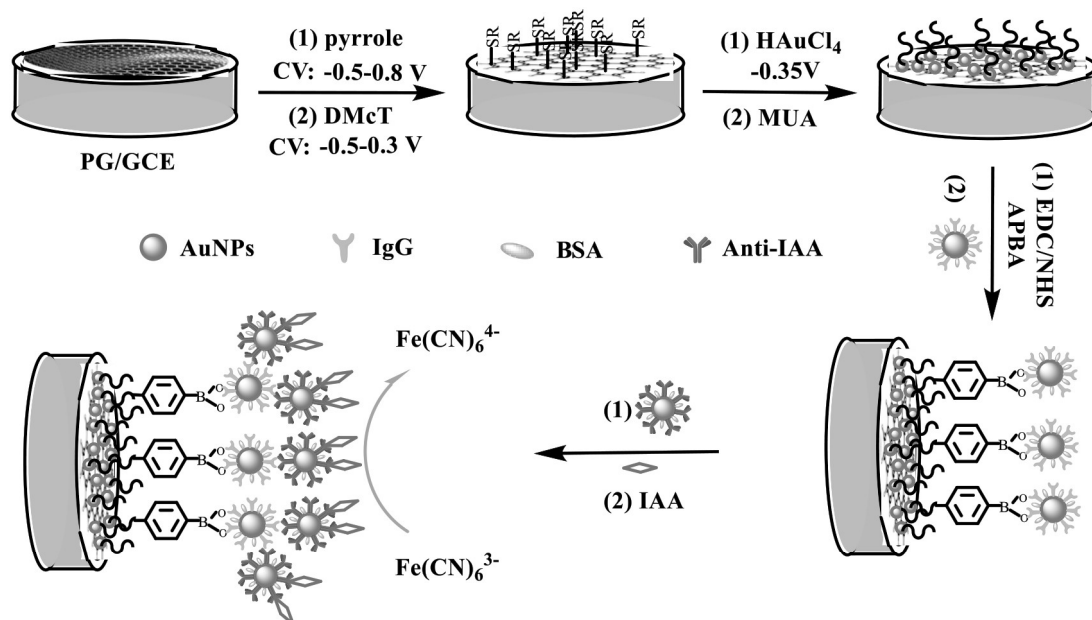


Fig. 8. Schematic illustration of the fabrication and detection process of the IAA electrochemical immunosensor. Reprinted with permission from (Su et al., 2020)

2.2.3 Non-antibody-based specific sensors

In immunoelectrochemical sensors, antibodies are the key reagent for specific recognition (Yin et al., 2016), but they are difficult to preserve and expensive. The high cost of antibodies and the difficulty in their preservation limit the practical application of immunoelectrochemical sensors. To overcome these shortcomings, researchers have explored other methods to achieve specificity. Immunoelectrochemical sensors based on aptamers and molecularly imprinted polymers have been increasingly studied. Molecularly imprinted polymers are ideal substitutes for antibodies. Ma et al. designed a highly selective electrochemical sensor for SA using molecularly imprinted polymers for recognition (Ma et al., 2017). Aptamers are single-stranded DNA or RNA that can compensate for the shortcomings of antibodies. Zhou et al constructed an electrochemical aptasensor (Zhou et al., 2018). As shown in Figure 9, the electrode was modified with AuNPs and MoS₂ nanosheets to improve its electron transfer efficiency. Zeatin could be captured by Y-type DNA, which was formed by hybridizing the aptamer and assistant DNA with probe DNA. Alkaline phosphatase (ALP), which can catalyze the hydrolysis of *p*-nitrophenylphosphate disodium (PNPP) to *p*-nitrophenol (PNP), could be modified on the electrode surface through biotin and avidin interactions. The presence of zeatin removed the ALP from the aptamer DNA terminals on the electrode surface, which led to a decrease in the oxidation signal of PNP. The linear range was from 50 pM to 50 nM, and the LOD reached 16.6 pM (S/N = 3).

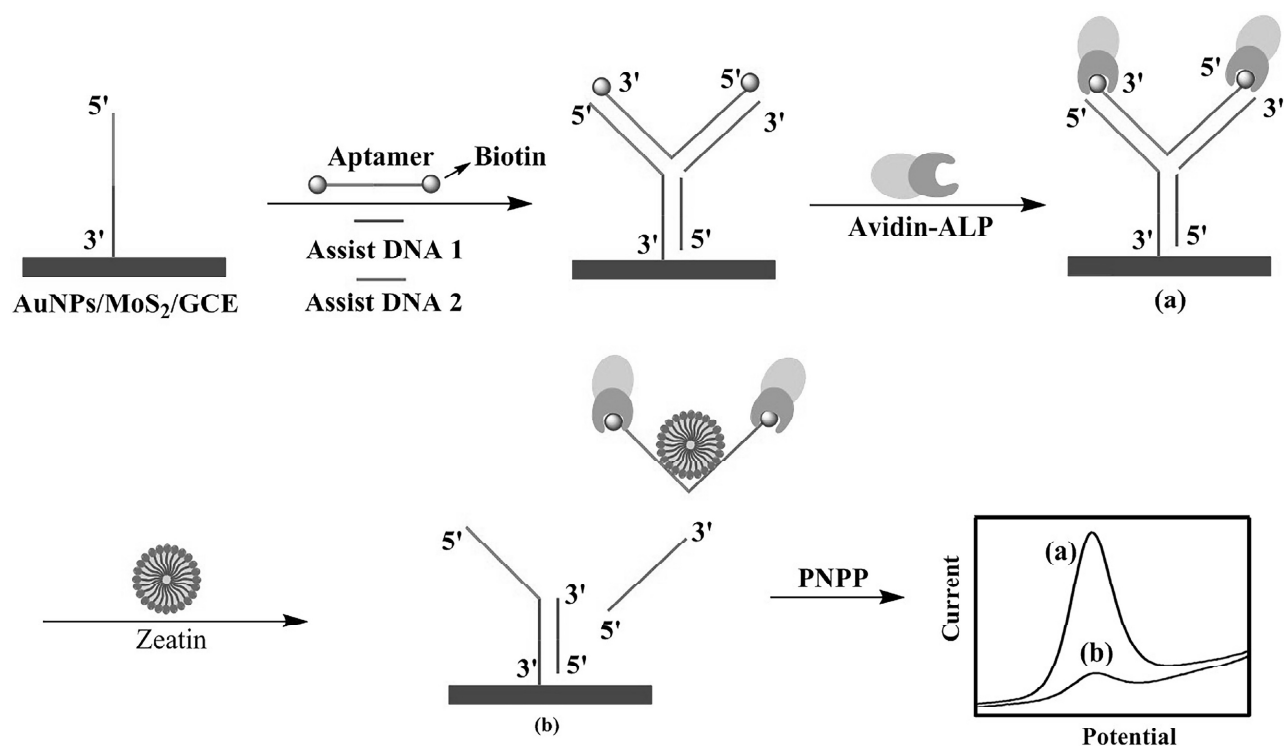


Fig. 9. Schematic representation of aptasensor fabrication and zeatin detection. Reprinted with permission from (Zhou et al., 2018)

2.3 PEC sensors for phytohormones

A PEC sensor applies photoirradiation as the excitation source to stimulate a photoactive material to produce carriers, which are separated and transmitted on the biointerface. PEC has the advantages of a low background signal and high sensitivity, which makes it suitable for the real-time, rapid detection of trace analytes. At present, it has been widely used in the detection of heavy metals (Li et al., 2014), proteins (B. Wang et al., 2018), DNA (Zhao et al., 2012), cells (Liu et al., 2015) and other targets. Due to the inherent mechanism of PEC analysis, in which it is difficult to distinguish the photocurrents generated by different photoactive materials during the measurement process, the ratio determination method used in electrochemistry should be used to eliminate external interference from the environment, instruments, human operation, etc.; however, this approach has rarely been reported in PEC analysis. In addition, the simultaneous determination of multiple samples by PEC remains to be studied. Photoactive materials with high photoelectric conversion efficiency play a key role in the construction of PEC biosensing systems. Graphite-like carbon nitride (g-C₃N₄) is a metal-free semiconductor that is nontoxic, easy to prepare, chemically and thermally stable, water soluble, and biocompatible; additionally, it has a relatively low band gap and responds to visible light. In many studies, it has been used as a photoactive material (Y. Wang et al., 2018; Yin et al., 2016). However, it suffers from the limitation of low photoelectric conversion efficiency. An effective strategy for improving sensitivity is to increase the adsorption of materials by doping and band-gap engineering (An et al., 2010). Photoactive materials based on heterojunctions can generate an enhanced photocurrent density by improving the light utilization efficiency and the efficient separation and transmission of photocarriers (Dong et al., 2017; Zhao et al., 2015; Sui et al., 2019). In addition to the use of photoactive materials, signal amplification strategies are an important means of improving sensitivity and include enzyme catalysis (Shu et al., 2015), hybridization chain reaction (C. Li et al., 2015) and rolling circle amplification (Zhuang et al., 2015). Cao et al. applied a novel signal amplification technique for the detection of prostate-specific antigen, in which GO-CuS@antibody₂ (Ab₂) conjugates acted as the signal amplification tag and ternary CdS@Au-g-C₃N₄ heterojunctions acted as the photoactive matrix (Cao et al., 2020). PEC sensors can improve their low sensitivity through different signal amplification strategies, but they still present challenges when detecting trace components in complex samples.

2.3.1 PEC immunosensors for phytohormones

A PEC immunosensor was first adopted for the analysis of phytohormones by B. Sun et al., in which 3-mercaptopropionic acid-stabilized CdS/reduced graphene oxide (MPA-CdS/RGO) nanocomposites were prepared (B. Sun et al., 2014). In this work, CdS was the photoactive material and possessed a band gap of ~2.4 eV, RGO was the electron-transport matrix and inhibited the recombination of electrons and holes, and MPA was the modifier that uniformly immobilized CdS and acted as a bridge to fix antibodies. The linear range of the above sensor was 0.1 to 1000 ng/mL, and it exhibited a low LOD of 0.05 ng/mL. The sensing mode was the change in steric hindrance caused by the formation of complexes in the process of biometric recognition, which led to a

change in the photocurrent signal.

Since many phytohormones coexist, detection targets are susceptible to other interferents. Thus, it is necessary to improve the specificity of PEC. Antibodies are the key reagent for specific recognition (Yin et al., 2016), but they are expensive and difficult to preserve. Taking advantage of aptamers, Wang et al. explored a PEC biosensor for zeatin detection based on a g-C₃N₄ and DNA aptamer, as shown in Figure 10 (Y. Wang et al., 2018). In the presence of zeatin, the biotin-labeled aptamer bound to the target zeatin to form a stable complex, causing the labeled aptamer to fall off the surface of the electrode and leaving a single-stranded DNA probe. After adding Exo I, the single-stranded DNA was further released from the electrode surface by enzymatic hydrolysis. With less biotin, less streptavidin was trapped on the electrode, which helped the electron receptors diffuse to the electrode surface to inhibit the recombination of photogenerated electron-hole pairs, resulting in a stronger photocurrent. Under optimal conditions, the linear range of this sensor was 0.1 to 100 nM, and it demonstrated a low detection limit of 0.031 nM (3σ).

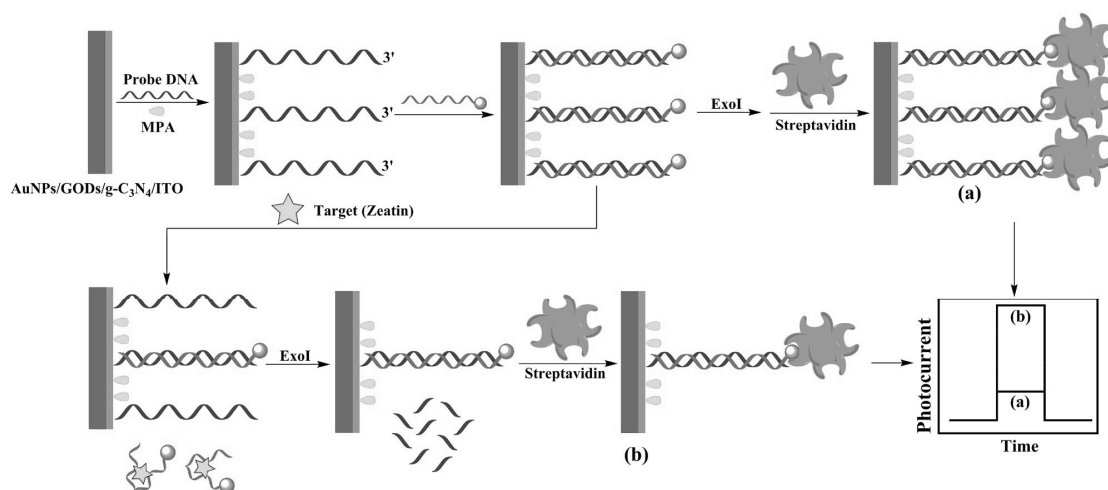


Fig. 10. Schematic diagram of PEC biosensor fabrication and zeatin detection based on a g-C₃N₄ and DNA aptamer. Reprinted with permission from (Y. Wang et al., 2018).

2.3.2 PEC sensors for microRNAs associated with phytohormones

MicroRNAs play a key role in the signaling pathway of phytohormones, so the adaptation of phytohormones to abiotic stress is often accompanied by changes in microRNAs. The concentration of miRNAs in plant tissues can be a selective and specific indicator of plant stress. The sensitivity and specificity of miRNA detection are necessary for understanding the interconnection between miRNAs and phytohormones. Li et al. developed a PEC sensor to detect miRNA-319a and evaluate miRNA expression levels in rice seedling leaves treated with different phytohormones (Li et al., 2018). As shown in Figure 11, the rolling circle, nicking enzyme and ALP catalytic amplification strategies were applied to generate exponential signal amplification. CuO-CuWO₄ was used as the photoactive material. A wide linear range of 1 fM to 0.1 nM was obtained for this sensor, and the detection limit was estimated to be 0.47 fM (S/N = 3).

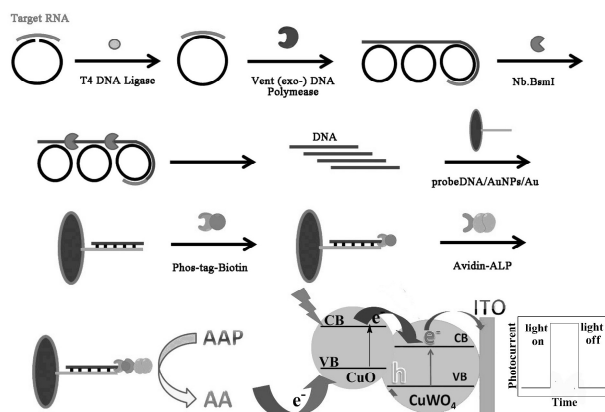


Fig. 11. Schematic illustration of the PEC sensor for microRNA detection. Reprinted with permission from (Li et al., 2018).

It can be concluded from the above literature that the application of photoelectrochemical sensors for detecting plant biomarkers has attracted the attention of researchers in recent years because the background current of photoelectrochemical sensors is low, which is particularly suitable for plants with complex detection environments. In addition, because aptamers are cheaper and easier to store than antibodies, they are replacing antibodies as specific recognition components in electrochemical sensors.

3. Different abiotic stress biomarkers for detection by electrochemical biosensors

To further understand the relationship between biomarkers and different abiotic stress factors, various methods have been used to detect changes in the biomarkers of plants treated with different abiotic stress factors, as shown in Table S2. Electrochemical sensors are a powerful tool to detect abiotic stresses. Thus, we discuss the application of electrochemical sensors to the detection of these abiotic stresses.

3.1 Heavy metal stress

If plants are exposed to heavy metal pollution for a long time, their yield and quality will decrease, which will eventually cause harm to human health. Therefore, the timely detection of heavy metals is important. Considering the disadvantages of atomic absorption spectrometry and inductively coupled plasma mass spectrometry, namely, the need for expensive instruments and skilled operators, electrochemical sensors are an ideal alternative. Based on the work of Cheng et al. (2018), in which vitronectin-like proteins (VNs) were utilized as biomarkers for detecting the effects of lanthanum on plant cells, Wang et al. constructed a novel immunoelectrochemical biosensor based on a GCE to monitor invisible damage to plant cells induced by cadmium [Cd(II)] or lead [Pb(II)] in a timely manner (X. Wang et al., 2019). As shown in Figure 12, the surface of the GCE was treated with L-cysteine (L-Cys) to form GCE-(L-Cys) through amino oxidation, and then anti-IgG-Au was fixed onto the surface of GCE-(L-Cys) via combination of the sulfhydryl group in L-Cys with the nano-Au particles in anti-IgG-Au. Finally, the protoplast, treated with anti-VN, was applied to the electrode. The linear dynamic ranges and the LODs are listed in Table S2.

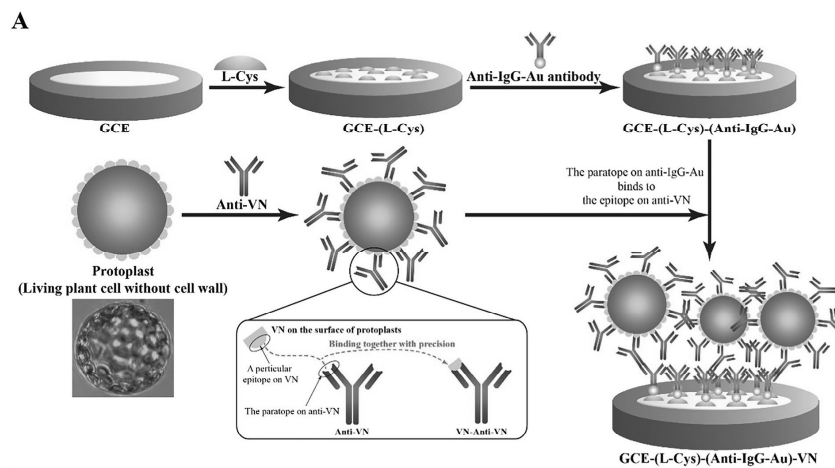


Fig. 12. Construction principle of the immunobiosensor (protoplasts: plant cells that have their cell wall entirely removed). Reprinted with permission from (X. Wang et al., 2019).

3.2 Salt stress

Salt stress is a natural factor that affects plant growth and crop yield. When the negative effects of salt stress are resisted, the relevant biomarkers in the plant body change. Researchers have examined different biomarkers to understand osmotic stress in plants.

Using IAA as a biomarker, H. Li et al. (2019) developed a disposable SS wire microelectrode that could detect IAA in soybean seedlings treated with different salt stress levels *in vivo*. The microelectrode was fabricated as shown in Figure 13. The linear range of this microsensors was 0.1–100,000 ng/mL, and the LOD (by voltammetry) reached 43 pg/mL. After a 36-hour salt treatment, the IAA level rose and then fell. They compared the results obtained by the developed microsensors *in vivo* with UPLC-MS results and confirmed that the developed microsensors were reliable for detecting IAA *in vivo*. Another group analyzed the levels of IAA and SA in continuous parts of whole pea seedlings under normal conditions and salinity with PADs and presented the results in the form of heatmaps (Sun et al., 2018). They found that IAA biosynthesis was not affected by salt stress but transport was negatively affected. However, the biosynthesis and transport of SA were both affected by salt stress.

When plants receive external salt stress, ROS can be induced, causing oxidative damage to proteins, DNA and lipids. Using hydrogen peroxide, a major reactive oxygen radical, as a biomarker, (Ren et al., 2013) constructed a direct electron transfer-based *in vivo* H₂O₂ sensor. The sensor was developed by modifying hemoglobin (Hb)-immobilized SWCNTs on the surface of CFUMEs. During the measurement of aloe leaves treated with salt, the hydrogen

peroxide level increased sharply after 12.5 hours of treatment, while during the measurement of aloe without salt stress, the hydrogen peroxide level remained stable throughout.

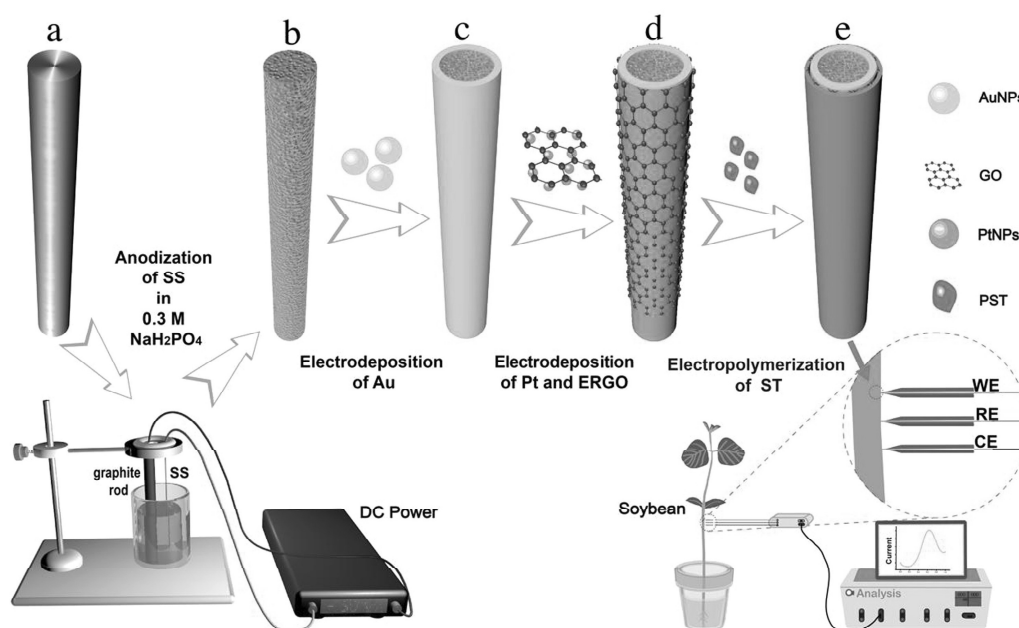


Fig. 13. Schematic illustration of the fabrication process of the SS microelectrode: bare SS (a), anodized SS (a-SS) (b), Au/a-SS (c), Pt-RGO/Au/a-SS (d), polymerized safranine T (PST)/Pt-ERGO/Au/a-SS (e). Reprinted with permission from (H. Li et al., 2019).

3.3 Heat stress

Based on the concept of the “Internet of Plants”, in which information is collected from the plant itself, Pandey et al. (2018) first reported a noninvasive and stimulus-specific assay of enzyme expression in plants. The sensing principle is based on a three-electrode microchip. As shown in Figure 14, the β -D-glucuronidase (GUS) enzyme catalyzed the substrate into β -glucuronide and P (either phenolphthalein or *p*-nitrophenol). The electroactive product P was oxidized on the working electrode, and the electrochemical signal was measured. For in situ sensing, the chip was clamped to the substrate injection side of the leaf and supported with polydimethylsiloxane (PDMS), as shown in Figure 15. The sensor showed better sensitivity for heat shock-induced cells than constitutive GUS-producing cells.

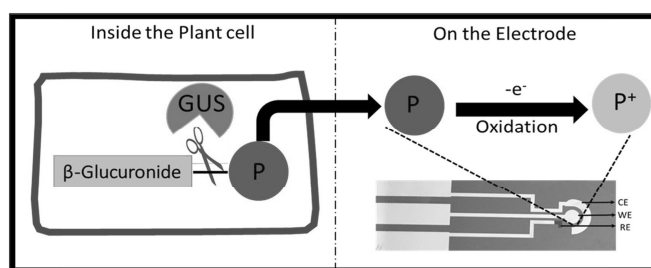


Fig. 14. Schematic of the GUS enzyme reaction inside the cell and oxidation of the enzyme product (P, either phenolphthalein or *p*-nitrophenol) onto the three-electrode chip. The electrodes were a Au working electrode (WE), a Au counter electrode (CE), and a Ag/AgCl reference electrode (RE). Reprinted with permission from (Pandey et al., 2018).

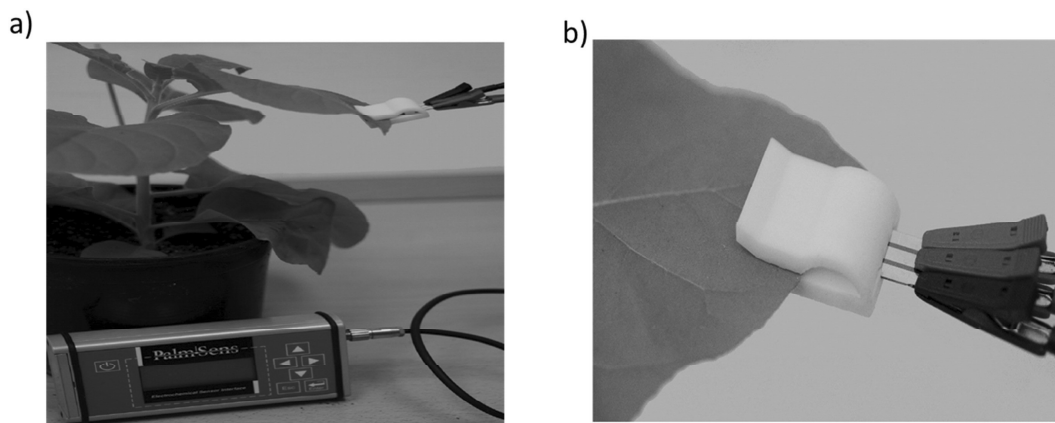


Fig. 15. a) Chip connected to a portable potentiostat and to leaves using a 3D printed chip holder and b) the 3D printed white polymer chip holder containing the chip in contact with the abaxial side of the leaf. Reprinted with permission from (Pandey et al., 2018).

4. Challenges and future perspectives

4.1 Challenges

This review focuses on research on electrochemical sensors for the detection of abiotic stress biomarkers, mainly including various phytohormones. The LOD of electrochemical sensors can reach several pg/mL or even lower, showing great potential for application in precision agriculture. However, practical applications still face some challenges.

4.1.1 Appropriate biomarkers

According to the research works listed above, plant hormones are important biomarkers for the study of abiotic stress. In addition to phytohormones, biomarkers associated with abiotic stress include polyamines (Gill and Tuteja, 2010), transcription factors (Lata and Prasad, 2011), proteins (Lee and Kang, 2020), and the secondary signals of plant hormones (Kazan, 2015). The physiological process of plants is often accompanied by changes in various biomarkers. Therefore, it remains challenging to select biomarkers that can distinguish between the severity of abiotic stress and the source of the stress to which crops are exposed.

4.1.2 Portable testing instrument

The use of ultramicroelectrodes or microchips could realize *in vivo* or noninvasive detection. Current studies mainly focus on the design of the components that generate the electrochemical signal, but the final reading of the signal depends mainly on unwieldy chemical workstations or potentiostats in the laboratory. More efforts are needed to develop an integrated sensing system to achieve portability of these devices. The limited development of high-efficiency, intelligent, portable and high-precision electrochemical instruments still restricts the practical application of electrochemical sensors in agriculture.

4.1.3 Practical application mode

Agriculture is a large system, and every plant is part of the system. The plant body includes roots, stems, branches, leaves and other tissues. In practical applications, the information obtained through the sensor needs to reflect the overall physiological status of the individual plant, and the information collected by all the sensors in the plants can reflect the status of the entire field system. However, different plants have different shapes and sizes, so it is urgent to solve the problem of how to implant electrochemical sensors into plants.

4.2 Future perspectives

Considering the development of electrochemical sensors and material science in nonplant applications, the following are future prospects for applications in plants.

4.2.1 Textile-based electrochemical sensors

Biosensors implanted into plants can realize real-time online monitoring of the physiological state of the plant. To improve the output performance of the sensor, the materials modifying the biosensor electrode should have good biocompatibility and stability in physiological environments. Therefore, the development of new biocompatible sensing materials can provide more opportunities for the *in vivo* monitoring of plants. (Coppedè et al., 2017) presented a biomimetic electrochemical transistor based on textile materials that was readily integrated into plant tissue to detect signs of abiotic stress *in vivo* and in real time by measuring the impedance of the conducting textiles that were inserted into the stem, as shown in Figure 16. Textile-based organic electrochemical transistors (OECTs) have the ability to convert ion signals in plants into electrical signals in circuits, so they are a simple means of measuring changes in ion concentrations in plant tubes. Moreover, conductive fabric yarns are flexible and structurally stable in complex environments (Tarabella et al., 2012). The same group also used this “bioristor” to monitor the effects of vapor pressure deficit (VPD) changes (Vurro et al., 2019). This sensor could provide a new way to analyze the mechanism of plant responses to abiotic stress.

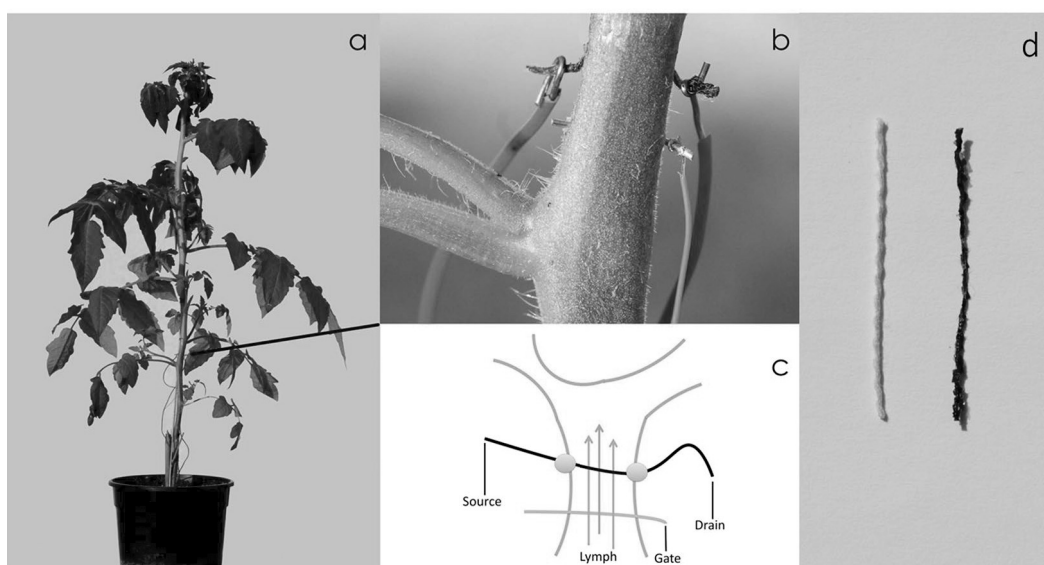


Fig. 16. (a) A bioristor integrated in a tomato plant. (b) Details of the textile device implantation and the silver gate connected through the plant stem. (c) Sketch of the proposed biosensor device showing the electrical connections Green lines: sketch of plant stems. Black line: textile thread. Gray line: gate electrode. Arrows: lymph flow. (d) Untreated cotton thread (left) and cotton thread functionalized with PEDOT:PSS (right). Reprinted with permission from (Coppedè et al., 2017).

4.2.2 Plant-wearable electrochemical sensors

Wearable sensors can be directly attached to the wearer for continuous, noninvasive and real-time monitoring. However, most wearable sensors have only been applied for human health assessment. Due to the good mechanical compatibility of wearable devices, they can be installed on soft surfaces. A wearable sensor can be applied to a plant for the real-time monitoring of its health and specific needs; thus, intervention measures can be taken to reduce damage to the plant before symptoms appear. Recently, scholars have designed and manufactured wearable devices and applied them to many tests in agricultural systems (Kim et al., 2019; Kim et al., 2020; Z. Li et al., 2019; Zhao et al., 2020; Lu et al., 2020). Mishra et al combined disposable polymer gloves with screen-printed electrodes to produce a flexible and stretchable wearable device to detect the threat of organophosphorus chemicals (Mishra et al., 2017). Jian Wu's group at Zhejiang University quickly prepared flexible sensors by writing with CS and graphite powder inks in a certain proportion on the solid surface of a Chinese brush plant, thereby allowing the pesticide content on the leaves to be measured *in situ* (Tang et al., 2015) and the plant growth to be monitored onsite (Tang et al., 2017). In regard to quantitative measurements, the team developed an all-in-one device that

integrated a sensor and signal reading circuit for nanoscale measurements in seconds (Tang et al., 2019), as shown in Figure 17.

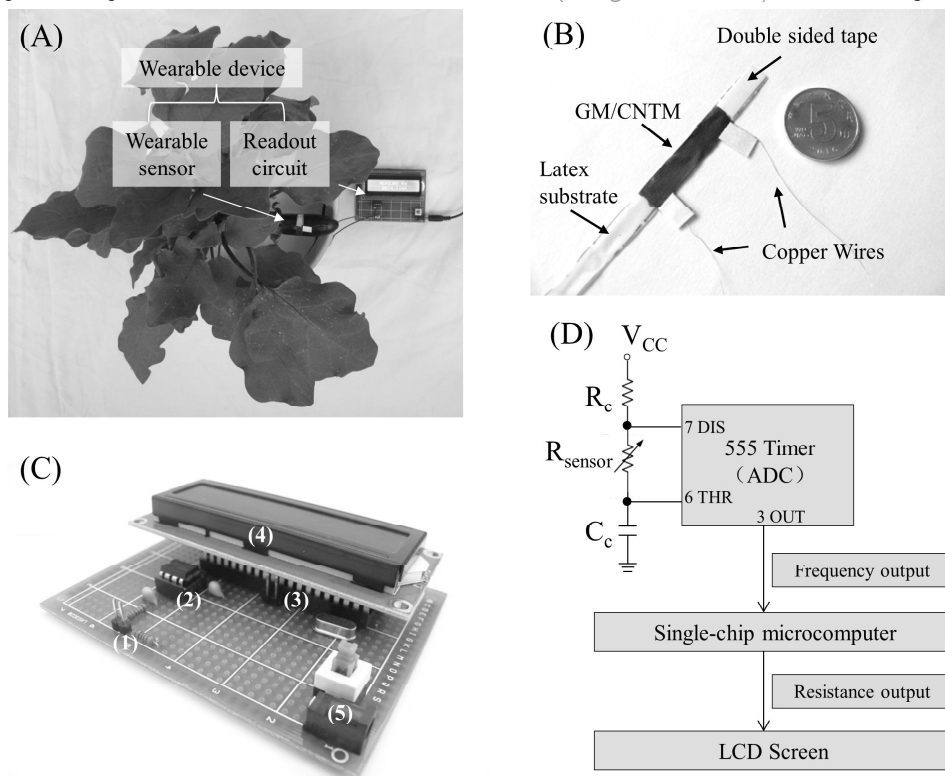


Fig. 17. Images and schematic illustration of the all-in-one wearable device for plant growth measurement. (A) Photograph of the device for plant growth monitoring. (B) Photograph of a wearable strain sensor. (C) Photograph of the homemade readout circuit. The main components were as follows: (1) sensor interface, (2) 555 timer, (3) single-chip microcomputer, (4) LCD1602 display and (5) power switch and interface. (D) System-level block diagram of the all-in-one device. TRIG (Trigger), OUT (Output), THR (Threshold) and DIS (Discharge) were the pinouts of the 555 timer. Reprinted with permission from (Tang et al., 2019).

4.2.3 Highly integrated electrochemical sensors

The point-of-need detection of plant biomarkers requires sample injection, sample processing, molecular recognition and signal conversion and output, among which sample injection and processing are key factors in the development of portable equipment. In paper-based microfluidic platforms, the capillary phenomenon is used to place samples in the test area, but this method has some limitations when dealing with complex liquids. These unit operations can be integrated onto a single chip by integrating microarray, microelectromechanical system (MEMS), and microfluidic technologies to utilize small sample sizes and achieve online, automatic monitoring of multiple samples. Bras et al developed a versatile and fully integrated hand-held device based on microfluidics for the detection of azelaic acid, a known biomarker for plant health (Bras et al., 2020), as shown in Figure 18.

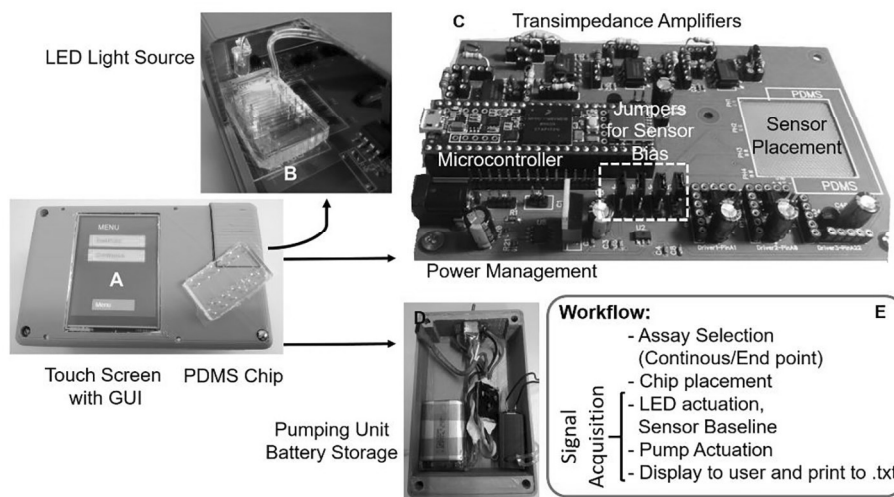


Fig. 18. Prototype system composition. On the outside of the box, a touch screen is available for user interaction (A), and in the upper right corner, there is a lid that allows placement of the microfluidic device in the sensing region for the transmission measurement (B). The prototype is comprised of a 14 x 8 cm

custom made PCB (C). Underneath the PCB are located the batteries as well as the peristaltic pump for fluidic handling (D). The workflow of the prototype is summarized (E). Reprinted with permission from (Bras et al., 2020).

5. Summary and Conclusions

In precision agriculture, it is important to monitor changes in the physiological markers of plants as early as possible, thereby allowing quick identification of the stress response and avoiding adverse effects on plant productivity and health. The electrochemical detection of plant hormones has been a topic of considerable laboratory research. To apply electrochemical detection technology to precision agriculture, electrochemical sensors are being developed with a focus on portability, disposability, and real-time monitoring, where the same device can simultaneously measure multiple biomarkers. However, electrochemical sensors applied in the field to realize in situ, in vivo and online measurements of plant physiological status are still subject to the following constraints, which are potential future research directions. First, due to the large size of plants, the in situ online measurement of biomarkers in different parts of plants remains challenging. Second, as the actual environment in which biomarkers exist is complex and different from the experimental environment, the simultaneous detection of multiple biomarkers still suffers difficulties in regard to anti-interference and specificity. In addition, current studies mainly focus on the variation trends of biomarkers in plants under different abiotic stresses, but the mechanisms behind the corresponding phenomena are not clear and need further investigation.

Overall, current methods such as microfluidic technology and computer technology need to be integrated to achieve desirable performance characteristics and make detection more intelligent and automatic. In addition, advances in wearable electronics should be facilely translated to plant wearable sensors, which would provide a friendly solution for in situ, online, real-time detection. We believe that the application of electrochemical sensors in agriculture can make the concept of the "Internet of Plants" a reality.

CRedit author statement

Zhilei Li: Writing - original draft, Writing - review & editing, Investigation.

Jianping Zhou: Conceptualization, Methodology, Writing -review & editing, Supervision, Project administration, Funding acquisition.

Tao Dong: Conceptualization, Methodology, Investigation, Writing - review & editing, Supervision.

Yan Xu: Conceptualization, Methodology.

Yukui Shang: Investigation.

Declaration of competing interests

The authors declare that they have no known competing financial interests or personal relationships that could have appeared to influence the work reported in this paper.

Acknowledgment

This work was mainly supported by the Huka brand promotion project KSHSY-2019-09-01, "Walnut mechanization and intelligent equipment research and development demonstration".

This project was also financially supported by the National Natural Science Foundation of China (Project Nos. 51965057, 51665055) and the Natural Science Foundation of Xinjiang Province of China (Project No. 2017D01C021). We also appreciate the support from the Xinjiang Walnut Industry Research Institute.

This work was also supported by RFF Forskningsfond Oslofjordfondet, Praktisk og effektiv oppfølging av KOLS-pasienter i kommunene (Project No. 285575) and the National Natural Science Foundation of China under Project No. 61531008.

Table 1: Summary of typical applications of electrochemical biosensors in phytohormone detection

Sensor type	Substance	Working electrode	LOD	Linear range	Ref
Direct electrochemical	IAA	Silicone OV-17 modified carbon paste electrode	0.053 µg/mL	Up to 0.6 µg/mL	(Hernández et al., 1994)
	IAA	CFUMEs	The authors studied the effects of accumulation time, potential, scan rate and pH on IAA detection and established the optimal conditions.		(Hernández et al., 1996)
	Dihydrozeatin (DHZ) and dihydrozeatin riboside (DHZR)	Carbon fiber microelectrode	DHZ: 46 ng/mL; DHZR: 153.0 ng/mL	DHZ: 15.0–45.0 ng/mL; DHZR: 20.0–600.0 ng/mL	(Blanco et al., 1999)
	IAA	PST-rGO/anodized graphite electrode	5.0×10^{-6} M	1.0×10^{-7} – 7.0×10^{-6} M	(Gan et al., 2011)
	Cis-jasmone	Electrodeposited Nafion film-modified GCE	4.0×10^{-7} mol/L	6.0×10^{-7} to 1.0×10^{-4} mol/L	(Dang et al., 2011)
	IAA and SA	GH/GCE	IAA: 1.42 µM; SA: 2.80 µM	IAA: 4–200 µM; SA: 4–200 µM	(Cao et al., 2019)
	IBA	Boron-doped diamond electrode	0.62 µmol/L	6.6×10^{-6} to 59×10^{-6} mol/L	(Chylková et al., 2019)
	Cis-Jasmone	MWCNT/Nafion/GCE	2.0×10^{-7} M	4.0×10^{-7} – 1.4×10^{-5} M	(Dang et al., 2012)
	IAA	Polyurethane composite electrode	26 µg/L	1.3×10^{-6} – 94.7×10^{-6} mol/L	(de Toledo and Vaz, 2007)
	IAA	Poly(hydroxymethylated-3,4-ethylenedioxythiophene)/G/O/GCE	DPV: 0.087 µmol/L; SWV: 0.033 µmol/L	DPV: 0.6–10 µmol/L; SWV: 0.05–40 µmol/L	(Feng et al., 2014)
	SA	Pencil trace/carbon tape/Indium tin oxide (ITO)	Not available	1.0×10^{-6} – 1.0×10^{-4} mol/L	(He et al., 2020)
	ABA	HDME	30 ng/mL	not available	(Hernández et al., 1997)
	IAA and SA	CB-MWCNT–Nafion/Fc/CB–MWNT/GCE	IAA: 1.99 mM; SA: 3.30 mM	IAA: 25–1000 mM; SA: 25–1000 mM	(Hu et al., 2020)
	IAA and SA	CMC-SWCNT-MMT/GCE	IAA: 0.002 µM; SA: 0.0063 µM	IAA: 0.005–0.3 µM and 0.3–70 µM; SA: 0.01–300 µM	(Lu et al., 2015)
	IBA	HDME	40 µg/L	40–320 µg/L	(Shen et al., 2013)
	SA	Au@Fe ₃ O ₄ -CS/GCEs	0.10 µM	1.0 µM–1.2 mM	(Sun et al., 2013)
	IAA and SA	MWCNTs/CS/GCE	0.1 µM	0.67 to 48.82 µM	(Sun et al., 2015)
	IAA and SA	PADs (oxygen plasma/MWCNTs/carbon tape/ITO)	Not available	Not available	(Sun et al., 2017)
	IAA+SA	PADs (oxygen plasma/GO/carbon tape/ITO)	Not available	Not available	(Sun et al., 2018)
	IAA+SA	PADs (oxygen plasma/MWCNTs/carbon tape/ITO)	Not available	Not available	(Wang et al., 2020)
	SA	PADs(oxygen plasma/MWCNTs/Nafion/carbon tape/ITO)	Not available	Not available	(L. J. Sun et al., 2014)
	IAA	Boron-doped diamond electrode	1.22 µM	5.0–50.0 µM	(Yardim and Erez, 2011)
	ABA	BIFE/PG	0.209 µM (55.24 ng/mL)	0.756–15.08 µM	(Yardim, 2011)
	IAA + kinetin	PG	IAA: 0.14 µM; kinetin: 0.11 µM	IAA: 0.5–2 µM, 2.5–10 µM; kinetin: 0.5–2 µM, 2.5–10 µM	(Yardim and Şentürk, 2011)

Molecular imprinted polymer	SA	Molecularly imprinted polymer/AuNPs-graphene-CS/GCE	1.3×10^{-10} mol/L	$5 \times 10^{-10} - 5 \times 10^{-5}$ mol/L	(Ma et al., 2017)
Immuno-sensor	ABA	Anti-ABA/Poly(<i>O</i> -phenylenediamine)/gold electrode	1 ng/mL	10–5000 ng/mL	(Li et al., 2010b)
	ABA	Anti-ABA/AuNPs/GCE	5 ng/mL	10 ng/mL to 10 ug/mL	(Wang et al., 2009)
	IAA	Anti-IAA IgG/sol-gel-alginate-carbon composite electrode	Not available	5–500 µg/mL	(Li et al., 2003)
Aptamer-based electrochemical biosensor	ABA	Anti-IAA/porous nanostructured gold film/GCE	0.1 ng/mL	0.5–5,000 ng/mL	(Li et al., 2008)
	IAA	Ab/AuNPs-HRP-IgG/APBA/AuNPs/graphene/GCE	5.5×10^{-10} M	1×10^{-9} - 5×10^{-6} M	(Zhou et al., 2013)
	IAA	Anti-IAA/AuNPs/PAGE/GCE	0.016 ng/mL	2×10^{-11} - 2×10^{-8} g/mL	(Su et al., 2019)
	IAA	AuNPs-anti-IAA/AuNPs-IgG/APBA/AuNPs/TPPy-PAGE/GCE	0.13 pg/mL	0.2–1000 pg/mL	(Su et al., 2020)
	IAA	AuNPs-anti-IAA/HRP-IgG-Fe ₃ O ₄ /APBA/AuNPs/GCE	0.018 ng/mL	0.02–500 ng/mL	(Yin et al., 2013)
	Zeatin	ALP/double-stranded DNA/AuNPs/MoS ₂ /GCE	16.6 pM	50–50000 pM	(Zhou et al., 2018)
PEC	Zearalenone (ZEA)	Gold/ZEA	0.017 ng/mL	0.01–1000 ng/mL	(Azri et al., 2020)
	microRNA	ALP/antibody/RNA-DNA-g-C ₃ N ₄ -AuNPs/ITO	2.26 fM	5–3000 fM	(Yin et al., 2016)
	Zeatin	AuNPs/graphene quantum dots/g-C ₃ N ₄ /ITO	0.031 nM	0.1–100 nM	(Y. Wang et al., 2018)
5-hydroxymethylcytosine (5 hmC)	5-hydroxymethylcytosine	ZnO/5-formylcytosine/g-C ₃ N ₄ /MoS ₂ /ITO	2.6 pM	0.01–200 nM	(Sui et al., 2019)
	sine (5 hmC)	Antibody-MPA-CdS/RGO/ITO	0.05 ng/mL	0.1–1000 ng/mL	(B. Sun et al., 2014)

Table S2: Summary of different abiotic stress detection methods

Abiotic stress type	Biomarker	Plant	Detection method	LOD	Linear range	Reference
Heavy metals	VN	<i>Arabidopsis thaliana</i> /soybean	Impedance	Cd: 18.5; Hg: 25.6 nmol/L	Cd: 45–210; Hg: 120–360 $\mu\text{mol/L}$	(X. Wang et al., 2019b)
Osmotic stresses	IAA	Soybean seedlings	Voltammetry	43 pg/mL	0.1–100,000 ng/mL	(H. Li et al., 2019)
	H ₂ O ₂	Aloe	Amperometry	4 μM	4.90–405 μM	(Ren et al., 2013)
	ABA	Rice leaves	LSPR	0.33 μM	5×10^{-7} – 5×10^{-5} M	(Wang et al., 2017)
	IAA+SA	Soybean seedlings	Radiometric electrochemistry	IAA: 1.99 mM; SA: 3.30 mM	IAA: 25–1000 mM SA: 25 m–1000 mM	(Hu et al., 2020)
	IAA+SA	Pea seedlings	Paper-based electrochemical voltammetry	Not available	Not available	(Sun et al., 2018)
Drought	Sly miRNA-1886	Tomato	Optical absorption ratio	2 fM	$0 \sim 10^4$ fM	(Asefpour Vakilian, 2019)
	Drought-responsive promoter	<i>Petunia hybrida</i>	Optical spectroscopy	Not available	Not available	(Chong et al., 2007)
Heat	GUS	Tobacco cell	Voltammetry	Substrate: pNPG 0.6 mM Substrate: PhG 0.1 mM	Substrate: pNPG 1.3–10.4 mM Substrate: PhG 0.2–2 mM	(Pandey et al., 2018)

References

- Alipour, E., Majidi, M.R., Saadatirad, A., Golabi, S.M., Alizadeh, A.M., 2013. *Electrochim. Acta* 91, 36–42.
- An, Y., Tang, L., Jiang, X., Chen, H., Yang, M., Jin, L., Zhang, S., Wang, C., Zhang, W., 2010. *Chem. - A Eur. J.* 16, 14439–14446.
- Asefpour Vakilian, K., 2019. *Plant Physiol. Biochem.* 145, 195–204.
- Azri, F.A., Eissa, S., Zourob, M., Chinnappan, R., Sukor, R., Yusof, N.A., Raston, N.H.A., Alhoshani, A., Jinap, S., 2020. *Microchim. Acta* 187–275.
- Ben Rejeb, I., Pastor, V., Mauch-Mani, B., 2014. Plant responses to simultaneous biotic and abiotic stress: Molecular mechanisms. *Plants* 3, 458–475.
- Blanco, M.H., Quintana, M.D.C., Hernández, L., 1999. *Fresenius. J. Anal. Chem.* 364, 254–260.
- Bonroy, K., Friedt, J.M., Frederix, F., Laureyn, W., Langerock, S., Campitelli, A., Sára, M., Borghs, G., Goddeeris, B., Declerck, P., 2004. *Anal. Chem.* 76, 4299–4306.
- Bras, E.J.S., Pinto, R.M.R., Chu, V., Fernandes, P., Conde, J.P., 2020. *IEEE Sens. J.* 1748, 1–1.
- Brunoud, G., Wells, D.M., Oliva, M., Larrieu, A., Mirabet, V., Burrow, A.H., Beeckman, T., Kepinski, S., Traas, J., Bennett, M.J., Vernoux, T., 2012. *Nature* 482, 103–106.
- Cao, J.T., Dong, Y.X., Ma, Y., Wang, B., Ma, S.H., Liu, Y.M., 2020. *Anal. Chim. Acta* 1106, 183–190.
- Cao, X., Zhu, X., He, S., Xu, X., Ye, Y., 2019. *Sensors* 19, 5483–5495.
- Chen, H., Guo, X.F., Zhang, H.S., Wang, H., 2011. *J. Chromatogr. B.* 879, 1802–1808.
- Cheng, M., Wang, L., Yang, Q., Huang, X., 2018. *Ecotoxicol. Environ. Saf.* 158, 94–99.
- Chong, J.P.C., Liew, O.W., Li, B.Q., Asundi, A.K., 2007. *Proc. of SPIE* 6535, 65350S–65350S–8.
- Chýlková, J., Janíková, L., Sedlák, M., Váňa, J., Šelešovská, R., 2019. *Monatshefte fur Chemie* 150, 443–449.
- Coppedè, N., Janni, M., Bettelli, M., Maida, C.L., Gentile, F., Villani, M., Ruotolo, R., Iannotta, S., Marmioli, N., Marmioli, M., Zappettini, A., 2017. *Sci. Rep.* 7, 1–9.
- Cui, L., Lu, M., Li, Y., Tang, B., Zhang, C. yang, 2018. *Biosens. Bioelectron.* 102, 87–93.
- Dang, X., Hu, C., Chen, Z., Wang, S., Hu, S., 2012. *Acta* 81, 239–245.
- Dang, X., Hu, C., Shen, D., Chen, Z., Hu, S., 2011. *J. Electroanal. Chem.* 657, 39–45.
- de Toledo, R.A., Vaz, C.M.P., 2007. *Microchem. J.* 86, 161–165.
- Deng, C., Pi, X., Qian, P., Chen, X., Wu, W., Xiang, J., 2017. *Anal. Chem.* 89, 966–973.
- Deng, J., Yu, P., Wang, Y., Mao, L., 2015. *Anal. Chem.* 87, 3080–3086.
- Dewitte, W., Van Onckelen, H., 2001. *Plant Growth Regul.* 33, 67–74.
- Dong, Y.X., Cao, J.T., Liu, Y.M., Ma, S.H., 2017. *Biosens. Bioelectron.* 91, 246–252.
- Fahad, S., Hussain, S., Matloob, A., Khan, F.A., Khaliq, A., Saud, S., Hassan, S., Shan, D., Khan, F., Ullah, Najeeb, Faiq, M., Khan, M.R., Tareen, A.K., Khan, A., Ullah, A., Ullah, Nasr, Huang, J., 2015. *Plant Growth Regul.* 75, 391–404.
- Feng, Q.M., Zhang, Q., Shi, C.G., Xu, J.J., Bao, N., Gu, H.Y., 2013. *Talanta* 115, 235–240.
- Feng, Z.L., Yao, Y.Y., Xu, J.K., Zhang, L., Wang, Z.F., Wen, Y.P., 2014. *Chinese Chem. Lett.* 25, 511–516.
- Gan, T., Hu, C., Chen, Z., Hu, S., 2011. *Talanta* 85, 310–316.
- Gao, F., Qian, Y., Zhang, L., Dai, S., Lan, Y., Zhang, Y., Du, L., Tang, D., 2015. *Biosens. Bioelectron.* 71, 158–163.
- Gill, S.S., Tuteja, N., 2010. *Plant Signal. Behav.* 5, 26–33.
- Gong, Z.Q., Sujari, A.N.A., Ab Ghani, S., 2012. *Electrochim. Acta* 65, 257–265.
- Graf, A., Smith, A.M., 2011. *Trends Plant Sci.* 16, 169–175.
- Gualandi, I., Scavetta, E., Zappoli, S., Tonelli, D., 2011. *Biosens. Bioelectron.* 26, 3200–3206.
- He, K.C., Wang, H.R., Yang, H., Sun, L.J., Liu, W., Bao, N., 2020. *Anal. Chim. Acta* 1120, 59–66.
- Hernández, L., Hernández, P., Patón, F., 1996. *Anal. Chim. Acta* 327, 117–123.
- Hernández, P., Dabrio-Ramos, M., Patón, F., Ballesteros, Y., Hernández, L., 1997. *Talanta* 44, 1783–1792.
- Hernández, P., Galán, F., Nieto, O., Hernández, L., 1994. *Electroanalysis* 6, 577–583.
- Hou, S., Zhu, J., Ding, M., Lv, G., 2008. *Talanta* 76, 798–802.
- Hu, Y., Wang, X., Wang, C., Hou, P., Dong, H., Luo, B., Li, A., 2020. *RSC Adv.* 10, 3115–3121.

- Huo, X.L., Qi, J.F., He, K.C., Bao, N., Shi, C.G., 2020. *Anal. Chim. Acta* 1124, 32–39.
- Jia, J., Chen, H.G., Feng, J., Lei, J.L., Luo, H.Q., Li, N.B., 2016. *Anal. Chim. Acta* 908, 95–101.
- Kalaji, H.M., Jajoo, A., Oukarroum, A., Brestic, M., Zivcak, M., Samborska, I.A., Cetner, M.D., Łukasik, I., Goltsev, V., Ladle, R.J., 2016. *Acta Physiol. Plant.* 38,102–112.
- Kariuki, J.K., 2012. *J. Electrochem. Soc.* 159, H747–H751.
- Kaur, G., Kumar, S., Nayyar, H., Upadhyaya, H.D., 2008. *J. Agron. Crop Sci.* 194, 457–464.
- Kazan, K., 2015. *Trends Plant Sci.* 20, 219–229.
- Khan, M.I.R., Fatma, M., Per, T.S., Anjum, N.A., Khan, N.A., 2015. *Front. Plant Sci.* 6, 1–17.
- Kim, J.J., Allison, L.K., Andrew, T.L., 2019. *Sci. Adv.* 5,1–9.
- Kim, J.J., Fan, R., Allison, L.K., Andrew, T.L., 2020. *Sci. Adv.* 6, 1–10.
- Kumar, A.A., Mishra, P., Kumari, K., Panigrahi, K.C.S., 2012. *Front. Biosci.* 4, 1315–1324.
- Lata, C., Prasad, M., 2011. *J. Exp. Bot.* 62, 4731–4748.
- Lee, K., Kang, H., 2020. *Int. J. Mol. Sci.* 21,4548–4595.
- Li, B., Yin, H., Zhou, Y., Wang, M., Wang, J., Ai, S., 2018. *Sensors Actuators, B Chem.* 255, 1744–1752.
- Li, C., Wang, H., Shen, J., Tang, B., 2015. *Anal. Chem.* 87, 4283–4291.
- Li, G., Lu, S., Wu, H., Chen, G., Liu, S., Kong, X., Kong, W., You, J., 2015. *J. Sep. Sci.* 38, 187–196.
- Li, H., Wang, C., Wang, X., Hou, P., Luo, B., Song, P., Pan, D., Li, A., Chen, L., 2019. *Biosens. Bioelectron.* 126, 193–199.
- Li, J., Tu, W., Li, H., Bao, J., Dai, Z., 2014. *Chem. Commun.* 50, 2108–2110.
- Li, J., Xiao, L.T., Zeng, G.M., Huang, G.H., Shen, G.L., Yu, R.Q., 2003. *Anal. Chim. Acta* 494, 177–185.
- Li, Q., Wang, R.Z., Huang, Z.G., Li, H.S., Xiao, L.T., 2010. *Chinese Chem. Lett.* 21, 472–475.
- Li, S., Zhu, A., Zhu, T., Zhang, J.Z.H., Tian, Y., 2017. *Anal. Chem.* 89, 6656–6662.
- Li, W., Qian, D., Wang, Q., Li, Y., Bao, N., Gu, H., Yu, C., 2016. *Sensors Actuators, B Chem.* 231, 230–238.
- Li, Y., Hong, M., Lin, Y., Bin, Q., Lin, Z., Cai, Z., Chen, G., 2012. *Chem. Commun.* 48, 6562–6564.
- Li, Y.W., Xia, K., Wang, R.Z., Jiang, J.H., Xiao, L.T., 2008. *Anal. Bioanal. Chem.* 391, 2869–2874.
- Li, Z., Paul, R., Ba Tis, T., Saville, A.C., Hansel, J.C., Yu, T., Ristaino, J.B., Wei, Q., 2019. *Nat. Plants* 5, 856–866.
- Liu, S., Cao, H., Wang, Z., Tu, W., Dai, Z., 2015. *Chem. Commun.* 51, 14259–14262.
- Lu, Q., Chen, L., Lu, M., Chen, G., Zhang, L., 2010. *J. Agric. Food Chem.* 58, 2763–2770.
- Lu, S., Bai, L., Wen, Y., Li, M., Yan, D., Zhang, R., Chen, K., 2015. *J. Solid State Electrochem.* 19, 2023–2037.
- Lu, Y., Xu, K., Zhang, L., Deguchi, M., Shishido, H., Arie, T., Pan, R., Hayashi, A., Shen, L., Akita, S., Takei, K., 2020. *ACS Nano* 14, 10966–10975.
- Ma, L.Y., Miao, S.S., Lu, F.F., Wu, M.S., Lu, Y.C., Yang, H., 2017. *Anal. Lett.* 50, 2369–2385.
- Ma, Z., Ge, L., Lee, A.S.Y., Yong, J.W.H., Tan, S.N., Ong, E.S., 2008. *Anal. Chim. Acta* 610, 274–281.
- Mishra, R.K., Hubble, L.J., Mart, A., Kumar, R., Bar, A., Kim, J., Musameh, M.M., Kyrtziz, I.L., Wang, J., 2017. *ACS Sens.* 2, 553–561
- Mishra, S., Kumar, S., Saha, B., Awasthi, J., Dey, M., Panda, S.K., Sahoo, L., 2016. Crosstalk between Salt, Drought, and Cold Stress in Plants: Toward Genetic Engineering for Stress Tolerance, in: Tuteja N., and Gill S. S. (Eds.), *Abiotic Stress Response in Plants*. Wiley-VCH Verlag GmbH & Co. KGaA, pp. 55–86.
- Müller, A., Dücking, P., Weiler, E.W., 2002. *Planta* 216, 44–56.
- Olsson, J., Claesson, K., Karlberg, B., Nordström, A.C., 1998. *J. Chromatogr. A* 824, 231–239.
- Pandey, R., Teig-Sussholz, O., Schuster, S., Avni, A., Shacham-Diamand, Y., 2018. *Biosens. Bioelectron.* 117, 493–500.
- Pengelly, W., 1977. *Planta* 136, 173–180.
- Petrek, J., Havel, L., Petrlova, J., Adam, V., Potesil, D., Babula, P., Kizek, R., 2007. *Russ. J. Plant Physiol.* 54, 553–558.
- Ren, K., Wu, J., Yan, F., Zhang, Y., Ju, H., 2015. *Biosens. Bioelectron.* 66, 345–349.
- Ren, Q.Q., Yuan, X.J., Huang, X.R., Wen, W., Zhao, Y. Di, Chen, W., 2013. *Biosens. Bioelectron.* 50, 318–324.
- Sah, S.K., Reddy, K.R., Li, J., 2016. *Front. Plant Sci.* 7:571.
- Santhiago, M., Kubota, L.T., 2013. *Sensors Actuators, B Chem.* 177, 224–230.
- Santhiago, M., Strauss, M., Pereira, M.P., Chagas, A.S., Bufon, C.C.B., 2017. *ACS Appl. Mater. Interfaces* 9, 11959–11966.
- Santhiago, M., Wydallis, J.B., Kubota, L.T., Henry, C.S., 2013. *Anal. Chem.* 85, 5233–5239.
- Schmelz, E.A., Engelberth, J., Alborn, H.T., O'Donnell, P., Sammons, M., Toshima, H., Tumlinson, J.H., 2003. *Proc. Natl.*

Acad. Sci. U. S. A. 100, 10552–10557.

Seo, H., Kriechbaumer, V., Park, W.J., 2016. *J. Plant Biol.* 59, 93–104.

Shen, Y., Li, X., Chen, W., Cheng, F., Song, F., 2013. *J. Plant Biochem. Biotechnol.* 22, 319–323.

Shi, M., Peng, Y., Zhou, J., Liu, B., Huang, Y., Kong, J., 2007. *Biosens. Bioelectron.* 22, 2841–2847.

Shu, J., Qiu, Z., Zhuang, J., Xu, M., Tang, D., 2015. *ACS Appl. Mater. Interfaces* 7, 23812–23818.

Su, Z., Cheng, Y., Xu, X., Wang, H., Xiao, L., Tang, D., Xie, Q., Qin, X., 2020. *Microchem. J.* 153, 104380.

Su, Z., Xu, X., Cheng, Y., Tan, Y., Xiao, L., Tang, D., Jiang, H., Qin, X., Wang, H., 2019. *Nanoscale* 11, 962–967.

Sui, C., Li, F., Wu, H., Yin, H., Zhang, S., Waterhouse, G.I.N., Wang, J., Zhu, L., Ai, S., 2019. *Biosens. Bioelectron.* 142, 111516–111522.

Sun, B., Chen, L., Xu, Y., Liu, M., Yin, H., Ai, S., 2014. *Biosens. Bioelectron.* 51, 164–169.

Sun, L., Liu, X., Gao, L., Lu, Y., Li, Y., Pan, Z., Bao, N., Gu, H., 2015. *Anal. Lett.* 48, 1578–1592.

Sun, L.J., Feng, Q.M., Yan, Y.F., Pan, Z.Q., Li, X.H., Song, F.M., Yang, H., Xu, J.J., Bao, N., Gu, H.Y., 2014. *Biosens. Bioelectron.* 60, 154–160.

Sun, L.J., Pan, Z.Q., Xie, J., Liu, X.J., Sun, F.T., Song, F.M., Bao, N., Gu, H.Y., 2013. *J. Electroanal. Chem.* 706, 127–132.

Sun, L.J., Xie, Y., Yan, Y.F., Yang, H., Gu, H.Y., Bao, N., 2017. *Sensors Actuators, B Chem.* 247, 336–342.

Sun, L.J., Zhou, J.J., Pan, J.L., Liang, Y.Y., Fang, Z.J., Xie, Y., Yang, H., Gu, H.Y., Bao, N., 2018. *Sensors Actuators, B Chem.* 276, 545–551.

Sun, M., Johnson, M.A., 2015. *RSC Adv.* 5, 55633–55639

Tang, J., Tang, D., Su, B., Li, Q., Qiu, B., Chen, G., 2011. *Electrochim. Acta* 56, 3773–3780.

Tang, W., Wu, J., Ying, Y., Liu, Y., 2015. *Anal. Chem.* 87, 10703–10707.

Tang, W., Yan, T., Ping, J., Wu, J., Ying, Y., 2017. *Adv. Mater. Technol.* 2, 1700021–1700025.

Tang, W., Yan, T., Wang, F., Yang, J., Wu, J., Wang, J., Yue, T., Li, Z., 2019. *Carbon.* 147, 295–302.

Tarabella, G., Villani, M., Calestani, D., Mosca, R., Iannotta, S., Zappettini, A., Coppedè, N., 2012. *J. Mater. Chem.* 22, 23830–23834.

Thimann, K. V., Skoog, F., 1940. *Am. J. Bot.* 27, 951–960.

Tuteja, N., 2007. *Plant Signal. Behav.* 2, 135–138.

Ueda, M., Bandurski, R.S., 1969. *Plant Physiol.* 44, 1175–1181.

Vine, J.H., Noiton, D., Plummer, J.A., Baleriola-Lucas, C., Mullins, M.G., 1987. *Plant Physiol.* 85, 419–422.

Vishwakarma, K., Upadhyay, N., Kumar, N., Yadav, G., Singh, J., Mishra, R.K., Kumar, V., Verma, R., Upadhyay, R.G., Pandey, M., Sharma, S., 2017. *Front. Plant Sci.* 8, 1–12.

Vurro, F., Janni, M., Coppedè, N., Gentile, F., Manfredi, R., Bettelli, M., Zappettini, A., 2019. *Sensors* 19, 4667–4670.

Wang, B., Cao, J.T., Dong, Y.X., Liu, F.R., Fu, X.L., Ren, S.W., Ma, S.H., Liu, Y.M., 2018. *Chem. Commun.* 54, 806–809.

Wang, H.R., Bi, X.M., Fang, Z.J., Yang, H., Gu, H.Y., Sun, L.J., Bao, N., 2019. *Sensors Actuators, B Chem.* 286, 104–110.

Wang, Q., Li, X., Tang, L., Fei, Y., Pan, Y., Sun, L., 2020. *J. Appl. Phycol.* 32, 485–497.

Wang, R., Li, Y., Li, Q., Shen, G., Xiao, L., 2009. *Anal. Lett.* 42, 2893–2904.

Wang, S., Li, W., Chang, K., Liu, J., Guo, Q., Sun, H., Jiang, M., Zhang, H., Chen, J., Hu, J., 2017. *PLoS One* 12, 1–13.

Wang, W., Vinocur, B., Altman, A., 2003. *Planta* 218, 1–14.

Wang, X., Cheng, M., Yang, Q., Wei, H., Xia, A., Wang, L., Ben, Y., Zhou, Q., Yang, Z., Huang, X., 2019. *Sci. Total Environ.* 697, 134097–134107.

Wang, Y., Zhou, Y., Xu, L., Han, Z., Yin, H., Ai, S., 2018. *Sensors Actuators, B Chem.* 257, 237–244.

Wrkruprh, I.R.U., Vlv, Q.D.O., Rklgh, L., Zkhq, S., Guliw, W.K.H., Lq, Y., Lqgl, U., Wkh, D., Zkhuh, S., Iudjphqwdwlrq, W.K.H., 2001. *Characteristics of HPLC Columns and Mass Spectra of LC-MS for Phytohormone Analysis* 5–10.

KOJIMA, Kiyohide, 2001. *JARQ*, 35, 149–154.

Wu, K., Sun, Y., Hu, S., 2003. *Sensors Actuators, B Chem.* 96, 658–662.

Wu, L., Zhang, X., Liu, W., Xiong, E., Chen, J., 2013. *Anal. Chem.* 85, 8397–8402.

Xi, Z., Zhang, Z., Sun, Y., Shi, Z., Tian, W., 2009. *Talanta* 79, 216–221.

Yardim, Y., 2011. *Rev. Anal. Chem.* 30, 37–43.

Yardim, Y., Erez, M.E., 2011. *Electroanalysis* 23, 667–673.

Yardim, Y., Şentürk, Z., 2011. *Turkish J. Chem.* 35, 413–426.

Yin, H., Shang, K., Meng, X., Ai, S., 2011. *Microchim. Acta* 175, 39–46.

Yin, H., Xu, Z., Zhou, Y., Wang, M., Ai, S., 2013. *Analyst* 138, 1851–1857.

Yin, H., Zhang, Q., Zhou, Y., Ma, Q., Liu, T., Zhu, L., Ai, S., 2011. *Electrochim. Acta* 56, 2748–2753.

Yin, H., Zhou, Y., Li, B., Li, X., Yang, Z., Ai, S., Zhang, X., 2016. *Sensors Actuators, B Chem.* 222, 1119–1126.

Yin, H., Zhou, Y., Meng, X., Tang, T., Ai, S., Zhu, L., 2011. *Food Chem.* 127, 1348–1353.

Yin, H., Zhou, Y., Xu, J., Ai, S., Cui, L., Zhu, L., 2010. *Anal. Chim. Acta* 659, 144–150.

Yin, Z., Liu, Y., Jiang, L.P., Zhu, J.J., 2011. *Biosens. Bioelectron.* 26, 1890–1894.

Yu, Z.G., Lai, R.Y., 2012. *Chem. Commun.* 48, 10523–10525.

Yue, L., Zhong, H., Zhang, L., 2012. *Electrochim. Acta* 76, 326–332.

Zhang, W. De, Xu, B., Hong, Y.X., Yu, Y.X., Ye, J.S., Zhang, J.Q., 2010. *J. Solid State Electrochem.* 14, 1713–1718.

Zhang, Y., Ge, S., Wang, S., Yan, M., Yu, J., Song, X., Liu, W., 2012. *Analyst* 137, 2176–2182.

Zhao, F., He, J., Li, X., Bai, Y., Ying, Y., Ping, J., 2020. *Biosens. Bioelectron.* 170, 112636–112643.

Zhao, M., Fan, G.C., Chen, J.J., Shi, J.J., Zhu, J.J., 2015. *Anal. Chem.* 87, 12340–12347.

Zhao, W.W., Yu, P.P., Shan, Y., Wang, J., Xu, J.J., Chen, H.Y., 2012. *Anal. Chem.* 84, 5892–5897.

Zhou, Y., Xu, Z., Wang, M., Meng, X., Yin, H., 2013. *Electrochim. Acta* 96, 66–73.

Zhou, Y., Yin, H., Wang, Y., Sui, C., Wang, M., Ai, S., 2018. *Analyst.* 143, 5185–5190

Zhuang, J., Tang, Dianyong, Lai, W., Xu, M., Tang, Dianping, 2015. *Anal. Chem.* 87, 9473–9480.

Zuo, X., Xiao, Y., Plaxco, K.W., 2009. *J. Am. Chem. Soc.* 131, 6944–6945.